ELSEVIER

Journal of Fluids and Structures 21 (2005) 629–664

JOURNAL OF FLUIDS AND STRUCTURES

www.elsevier.com/locate/jfs

Pipes conveying pulsating fluid near a 0:1 resonance: Local bifurcations

R.J. McDonald[a], N. Sri Namachchivaya[b,*]

[a]*Boeing Satellite Systems, Inc., El Segundo, CA 90245, USA*
[b]*Department of Aerospace Engineering, University of Illinois at Urbana–Champaign, Urbana, IL 61801, USA*

Received 28 July 2004; accepted 27 July 2005

Abstract

We study the local bifurcation behavior of parametrically excited pipes conveying fluid near a 0:1 resonance. A major goal of the analysis is to understand how energy may be transferred from the high-frequency mode to the low-frequency mode in these systems. We study the bifurcations of pipe systems, focusing on the subharmonic resonance case. We calculate the stability of the trivial solution, the bifurcating single-mode branches and their stability, and the existence of multi-mode or periodic solutions. Regions where energy transfer may occur from high- to low-frequency modes are identified. The numerical bifurcation analysis software AUTO97 is used to support the analytical results.

1. Introduction

The problem of a supported pipe conveying pulsating fluid may model the nonlinear dynamics of a propellant line carrying fluid with a nonconstant flow rate. Pipes conveying fluid may also be found in boilers, nuclear reactors, heat exchangers, and steam generators. The primary goal of this and the second part (McDonald and Namachchivaya, 2005) of the research is to investigate the local and global dynamics of parametrically excited pipes conveying fluid near a 0:1 resonance.

When the pipe oscillates, the flow of fluid through the pipe introduces a gyroscopic or Coriolis force which is proportional to the fluid velocity. For small flow velocities, there is little coupling between the fluid and the structure. Centrifugal forces in the pipe act in much the same way as compressive forces do in a beam. Hence, increasing the fluid velocity decreases the effective stiffness of the pipe system, and may lead to buckling, also known as divergence. The Coriolis forces act to restabilize the pipe after divergence before flutter finally destabilizes the pipe. For an undamped system with no external tension or gravity, the classical result is that divergence of the first mode occurs at a dimensionless critical velocity of $u_c = \pi$.

There are a multitude of boundary conditions that are possible for pipes conveying fluid. Two common sets of boundary conditions are supported boundary conditions (simply supported or clamped), and cantilevered boundary conditions. For undamped, supported pipes, the only source of energy input is the fluid dynamic forces. However, over the course of any periodic motion of the pipe, the work done by these forces sums to zero, due to the fact that the displacement at both ends of the pipe is zero (Benjamin, 1961). Thus, supported pipes are conservative systems in the

*Corresponding author. Tel.: +1 217 333 2651; fax: +1 217 244 0720.
E-mail address: navam@uiuc.edu (N.S. Namachchivaya).

0889-9746/$ - see front matter © 2005 Published by Elsevier Ltd.
doi:10.1016/j.jfluidstructs.2005.07.019

absence of frictional forces. Cantilevered pipes, on the other hand, are nonconservative systems, since the displacement of the pipe at one end is nonzero, and hence the energy change in the pipe is nonzero. Another difference between these two sets of boundary conditions is that systems with supported boundary conditions destabilize through divergence, i.e., a simple bifurcation, while systems with cantilevered boundary conditions destabilize through flutter, i.e., a Hopf bifurcation.

A review of much of the work that has been done on this problem is given by Paidoussis and Li (1993). Some of the earliest work on pipes conveying fluid was done by Ashley and Haviland (1950), who attempted to explain vibrations in the Trans-Arabian Pipeline. The earliest studies of the linear stability of pipes supported at both ends were done in the early 1950s by Feodos'ev (1951), Housner (1952), and Niordson (1953). Other important work on the linear stability of this problem was done by Benjamin (1961), and Paidoussis and Issid (1974). The first study on the nonlinear dynamics of pipes conveying steady fluid flow was done by Thurman and Mote (1969), who showed that the importance of nonlinearities increases as the flow velocity becomes larger. Other important nonlinear studies of this problem include Holmes (1977), Ch'ng (1978) and Rousselet and Herrmann (1977). Most of these studies considered only steady-flow velocities. Work on the problem of pipes with parametrically excited flow velocities has been done by Paidoussis and Sundararajan (1975), Ariaratnam and Namachchivaya (1986), Namachchivaya (1989), and Namachchivaya and Tien (1989a,b).

In this paper, we study the local bifurcations of simply supported damped pipe systems *near the critical velocity* u_c, when the fluid velocity is also pulsating. The goal of our analysis is to understand the effect that the forcing and damping has on this gyroscopic system in the neighborhood of the 0:1 critical point. We determine the stability of the trivial solution, the location and type of primary bifurcation points, the nature of any bifurcating solutions, and the location and type of any secondary bifurcation points and branches. In addition to an analytical analysis, we will use the numerical bifurcation package AUTO97 (Doedel et al., 1997) to understand the dynamics of the system for more complicated systems. For simplicity, we concentrate on the subharmonic resonance case, since the lack of coupling between the modes from the forcing makes analytical solution of the bifurcating branches simpler. Another goal of our analysis is to understand where energy transfer can occur from the high-frequency second mode to the low-frequency first mode.

In Section 2, we present the finite-dimensional equations of motion for a pipe conveying fluid with a parametrically excited flow rate. The true continuum model is a PDE and it is derived in the appendix. The parametric excitation enters the system through a periodically pulsating fluid flow rate, given by $u = u_0(1 + \cos \nu t)$. We also include dissipation through Kelvin–Voigt damping, both linear and nonlinear. In Section 3, We introduce unfolding parameters and detuning parameters to observe the behavior of the system near critical states. We derive the equations of motion in both Lagrangian and Hamiltonian form. In Section 4, we calculate the normal form for the pipe system near the critical point at which the system possesses a nonsemisimple double zero eigenvalue. Bifurcation parameters are introduced into the equations off motion to capture the behavior of the system near the critical 0:1 resonance, and near two critical forcing frequencies. In Section 5, we study the local dynamics of the parametrically excited pipe. We also attempt to understand how the presence of damping, linear and nonlinear, interacts with the forcing. We identify various fixed points and periodic solutions for the system, and determine the stability and bifurcation behavior of these equilibria. The analytical analysis is complemented by the use of the numerical bifurcation package AUTO97 (Doedel et al., 1997). Finally in Section 6, we summarize the results and interpret them in terms of the physical motion of pipe conveying pulsating fluid.

2. Finite-dimensional equations of motion

The continuum equation of motion of a simply supported pipe (pinned–pinned) conveying fluid is given in the appendix. Standard Galerkin-type projections allow us to approximate this by a more tractable finite-dimensional dynamical system. In the Galerkin procedure for gyroscopic systems, it is essential to take at least two modes of the amplitude of the displacement for a good approximation; the result is a system of second-order equations (see the appendix)

$$\ddot{\mathbf{q}} + (\bar{E}^* \Lambda + a_2 B)\dot{\mathbf{q}} + (\Lambda + a_0 C - a_1 D)\mathbf{q} + f(\mathbf{q}, \dot{\mathbf{q}}) = \mathbf{0},$$

where $\Lambda = \operatorname{diag}\{\lambda_1^4, \lambda_2^4\}$, and the cubic nonlinear terms are given by

$$f(\mathbf{q}, \dot{\mathbf{q}}) = \begin{bmatrix} f_1(\mathbf{q}, \dot{\mathbf{q}}) \\ f_2(\mathbf{q}, \dot{\mathbf{q}}) \end{bmatrix}$$

and

$$f_s(\mathbf{q},\dot{\mathbf{q}}) = -\kappa(-c_{11}q_1^2 - 2c_{12}q_1q_2 - c_{22}q_2^2)\,(c_{s1}q_1 + c_{s2}q_2) - \sigma(-c_{11}q_1\dot{q}_1 - c_{22}q_2\dot{q}_2)\,(c_{s1}q_1 + c_{s2}q_2).$$

2.1. Harmonically perturbed axial flow

We now assume that the axial velocity of the flow is harmonically perturbed, $u = u_0(1 + \mu f(t))$. If we assume that the forcing and damping are small, i.e.,

$$\mu = \varepsilon h, \quad \bar{E}^* = \varepsilon\xi^*,$$

where ε is a small parameter, then the coefficients (a_1, a_2, a_3) from (20) become

$$a_0 = u_0^2 + 2\varepsilon h u_0^2 f(t) + \varepsilon^2 u_0^2 h^2 f^2(t) - \bar{T} + \varepsilon M_r h u_0 \dot{f}(t),$$
$$a_1 = \varepsilon M_r h u_0 \dot{f}(t),$$
$$a_2 = 2M_r u_0(1 + \varepsilon h f(t)).$$

We also note that $\sigma = 2\varepsilon\zeta^*\kappa$. The equation of motion then becomes [see Namachchivaya and Tien (1989b)]

$$\ddot{\mathbf{q}} + 2M_r u_0 B\dot{\mathbf{q}} + (\Lambda + (u_0^2 - \bar{T})C)\mathbf{q} + f(\mathbf{q},\dot{\mathbf{q}}) = \varepsilon h\{-M_r u_0 \dot{f}(t)(C - D) - (2u_0^2 f(t))C\}\mathbf{q} - \varepsilon h\{(2M_r u_0 f(t))B\}\dot{\mathbf{q}} - \varepsilon\zeta^*\Lambda\dot{\mathbf{q}}.$$

2.2. Pinned–pinned boundary conditions

If we now specify that the pipe has pinned–pinned boundary conditions, then we can determine the modal functions Φ_j and hence the coefficients of the matrices B, C, and D. We choose the modal functions $\Phi_j(\xi) = \sqrt{2}\sin j\pi\xi$, which determines the coefficients $c_{11} = -\pi^2$, $c_{22} = -4\pi^2$, $c_{12} = c_{21} = 0$, $d_{11} = -\pi^2/2$, $d_{22} = -2\pi^2$, $d_{12} = \frac{64}{9}$, $d_{21} = \frac{16}{9}$, $\lambda_1 = \pi$, $\lambda_2 = 2\pi$, and $b_{21} = \frac{8}{3}$. We can then write the matrices B, C, and D as

$$B = \begin{bmatrix} 0 & -\frac{8}{3} \\ \frac{8}{3} & 0 \end{bmatrix}, \quad C = \begin{bmatrix} -\pi^2 & 0 \\ 0 & -4\pi^2 \end{bmatrix}, \quad D = \begin{bmatrix} -\frac{\pi^2}{2} & \frac{64}{9} \\ \frac{16}{9} & -2\pi^2 \end{bmatrix}$$

and the equations of motion in the simpler form

$$\ddot{\mathbf{q}} + 2G\dot{\mathbf{q}} + K\mathbf{q} = \varepsilon(-hD_1\mathbf{q} - hD_2\dot{\mathbf{q}} - \zeta^*\Lambda\dot{\mathbf{q}} - g(\mathbf{q})\mathbf{q}), \tag{1}$$

where

$$G = M_r u_0 B = \frac{8}{3}M_r u_0 \begin{bmatrix} 0 & -1 \\ 1 & 0 \end{bmatrix},$$

$$K = \Lambda + (u_0^2 - \bar{T})C = \begin{bmatrix} \pi^4 - (u_0^2 - \bar{T})\pi^2 & 0 \\ 0 & 16\pi^4 - 4(u_0^2 - \bar{T})\pi^2 \end{bmatrix} = \begin{bmatrix} \omega_1^2 & 0 \\ 0 & \omega_2^2 \end{bmatrix},$$

$$g(\mathbf{q},\dot{\mathbf{q}}) = \begin{bmatrix} g_1(\mathbf{q},\dot{\mathbf{q}}) \\ g_2(\mathbf{q},\dot{\mathbf{q}}) \end{bmatrix} = \begin{bmatrix} \kappa\pi^2(\pi^2 q_1^2 + 4\pi^2 q_2^2) + 2\varepsilon\zeta^*\kappa\pi^2(\pi^2 q_1\dot{q}_1 + 4\pi^2 q_2\dot{q}_2) \\ 4\kappa\pi^2(\pi^2 q_1^2 + 4\pi^2 q_2^2) + 8\varepsilon\zeta^*\kappa\pi^2(\pi^2 q_1\dot{q}_1 + 4\pi^2 q_2\dot{q}_2) \end{bmatrix},$$

$$D_1 = M_r u_0 \dot{f}(t)\begin{bmatrix} -\frac{\pi^2}{2} & -\frac{64}{9} \\ -\frac{16}{9} & -2\pi^2 \end{bmatrix} + 2u_0^2 f(t)\begin{bmatrix} -\pi^2 & 0 \\ 0 & -4\pi^2 \end{bmatrix} = D_{1,s}\dot{f}(t) + D_{1,c}f(t),$$

$$D_2 = \frac{16}{3}M_r u_0 f(t)\begin{bmatrix} 0 & -1 \\ 1 & 0 \end{bmatrix} = D_{2,c}f(t)$$

and $\Lambda = \mathrm{diag}\{\lambda_1^4, \lambda_2^4\}$. The matrix K will be diagonal for the boundary conditions considered here. However, if this is not the case, then K can be diagonalized with an additional transformation.

3. Hamiltonian formulation

The Lagrangian function for the unperturbed system is given by

$$\begin{aligned}\mathscr{L} &= \tfrac{1}{2}\dot{\mathbf{q}}^{\mathrm{T}}\dot{\mathbf{q}} + \dot{\mathbf{q}}^{\mathrm{T}}G\mathbf{q} - \tfrac{1}{2}\mathbf{q}^{\mathrm{T}}K\mathbf{q} - U(\mathbf{q})\\ &= \tfrac{1}{2}(\dot{q}_1^2 + \dot{q}_2^2) + \tfrac{16}{3}M_r u_0(\dot{q}_2 q_1 - \dot{q}_1 q_2) - \tfrac{1}{2}(\omega_1^2 q_1^2 + \omega_2^2 q_2^2) - U(q_1, q_2),\end{aligned}$$

where ω_1 and ω_2 are given by

$$\omega_1^2 = \pi^2(\pi^2 - (u_0^2 - \bar{T})), \quad \omega_2^2 = 4\pi^2(4\pi^2 - (u_0^2 - \bar{T}))$$

and

$$U(\mathbf{q}) = \frac{\kappa\pi^4}{4}(q_1^2 + 4q_2^2)^2$$

is the nonlinear potential term.

3.1. Hamiltonian equations of motion

The generalized momentum is given by $\mathbf{p} = \partial\mathscr{L}/\partial\dot{\mathbf{q}} = \dot{\mathbf{q}} + G\mathbf{q}$, and hence $\dot{\mathbf{q}} = \mathbf{p} - G\mathbf{q}$. The Hamiltonian function is then given by

$$\begin{aligned}H(\mathbf{q},\mathbf{p}) &= \mathbf{p}^{\mathrm{T}}(\mathbf{p} - G\mathbf{q}) - \frac{1}{2}(\mathbf{p} - G\mathbf{q})^{\mathrm{T}}(\mathbf{p} - G\mathbf{q}) - (\mathbf{p} - G\mathbf{q})^{\mathrm{T}}G\mathbf{q} + \tfrac{1}{2}\mathbf{q}^{\mathrm{T}}K\mathbf{q} + U(\mathbf{q})\\ &= \tfrac{1}{2}(p_1^2 + p_2^2) + \tfrac{8}{3}M_r u_0(p_1 q_2 - p_2 q_1) + \tfrac{1}{2}(\bar{\omega}_1^2 q_1^2 + \bar{\omega}_2^2 q_2^2) + H_1(\mathbf{q},\mathbf{p}),\end{aligned}$$

where the nonlinear Hamiltonian term $H_1(\mathbf{q},\mathbf{p})$ is defined as

$$H_1(\mathbf{q},\mathbf{p}) \stackrel{\mathrm{def}}{=} \frac{\kappa\pi^4}{4}(q_1^2 + 4q_2^2)^2. \tag{2}$$

The two quantities $\bar{\omega}_1$ and $\bar{\omega}_2$ are defined as

$$\begin{aligned}\bar{\omega}_1^2 &= \pi^2(\pi^2 - (u_0^2 - \bar{T})) + \tfrac{64}{9}M_r^2 u_0^2 = \omega_1^2 + g_{21}^2,\\ \bar{\omega}_2^2 &= 4\pi^2(4\pi^2 - (u_0^2 - \bar{T})) + \tfrac{64}{9}M_r^2 u_0^2 = \omega_2^2 + g_{21}^2.\end{aligned}$$

The Hamiltonian equations of motion are then given by

$$\dot{\mathbf{x}} = A\mathbf{x} + JDH_1(\mathbf{x}) + \varepsilon\{h(\dot{f}(t)D_s + f(t)D_c - \zeta^* D_d)\}\mathbf{x} - \varepsilon\zeta^* F(\mathbf{x}), \tag{3}$$

where $\mathbf{x} = [q_1\ q_2\ p_1\ p_2]^{\mathrm{T}}$ and

$$A = \begin{bmatrix} 0 & \frac{8}{3}M_r u_0 & 1 & 0\\ -\frac{8}{3}M_r u_0 & 0 & 0 & 1\\ -\bar{\omega}_1^2 & 0 & 0 & \frac{8}{3}M_r u_0\\ 0 & -\bar{\omega}_2^2 & -\frac{8}{3}M_r u_0 & 0 \end{bmatrix}, \tag{4}$$

$$F(\mathbf{x}) = \begin{bmatrix} 0\\ 0\\ f_1(\mathbf{q},\mathbf{p})\\ f_2(\mathbf{q},\mathbf{p}) \end{bmatrix} = \begin{bmatrix} 0\\ 0\\ 2\kappa\pi^2\left(\pi^2 q_1\left(p_1 + \frac{8}{3}M_r u_0 q_2\right) + 4\pi^2 q_2\left(p_2 - \frac{8}{3}M_r u_0 q_1\right)\right)q_1\\ 8\kappa\pi^2\left(\pi^2 q_1\left(p_1 + \frac{8}{3}M_r u_0 q_2\right) + 4\pi^2 q_2\left(p_2 - \frac{8}{3}M_r u_0 q_1\right)\right)q_2 \end{bmatrix}, \tag{5}$$

$$D_s = \begin{bmatrix} 0 & 0\\ -D_{1,s} & 0 \end{bmatrix}, \quad D_c = \begin{bmatrix} 0 & 0\\ -D_{1,c} + D_{2,c}G & -D_{2,c} \end{bmatrix}, \tag{6}$$

$\Lambda = \text{diagonal}\{\lambda_1^4, \lambda_2^4\} = \{\pi^4, 16\pi^4\}$ and

$$D_d = \begin{bmatrix} 0 & 0 \\ \Lambda G & \Lambda \end{bmatrix}. \tag{7}$$

Eq. (3) represents the equations of motion (Hamiltonian form) for a two-mode truncation of the pipe conveying fluid.

3.2. Transformation of unperturbed linear matrix to normal form

We first transform the matrix A into its simplest form, i.e., a normal form. The eigenvalues of A are

$$\pm i\sqrt{\tfrac{64}{9}M_r^2u_0^2 + \tfrac{1}{2}(\bar{\omega}_1^2 + \bar{\omega}_2^2) \mp \sqrt{\tfrac{128}{9}M_r^2u_0^2(\bar{\omega}_1^2 + \bar{\omega}_2^2) + \tfrac{1}{4}(\bar{\omega}_1^2 - \bar{\omega}_2^2)^2}}.$$

We wish to study the system when it possesses a pair of zero eigenvalues. There are two cases to consider:

(i) $u_0^{c,1} = 3\bar{\omega}_1/8M_r$. In this case, the critical flow velocity is given by $u_0^{c,1} = \sqrt{\pi^2 + \bar{T}}$;
(ii) $u_0^{c,2} = 3\bar{\omega}_2/8M_r$. In this case, the critical flow velocity is given by $u_0^{c,1} = \sqrt{4\pi^2 + \bar{T}}$.

Thus, if $\bar{T} = 0$, we recover the familiar result that the pipe system has double zero eigenvalues at $u_0 = \pi$ and $u_0 = 2\pi$. We also note that in order for critical flow velocities to exist, we must have $\bar{T} > -\pi^2$ (for $u_0^{c,1}$) or $\bar{T} > -4\pi^2$ (for $u_0^{c,2}$). These limits correspond to the compressive buckling loads of a pipe without fluid flow. Thus, if the compressive load is large enough, than these critical flow velocities do not exist, since the pipe is unstable even without the presence of fluid flow.

For the pipe, the behavior of the eigenvalues as the flow velocity u_0 is varied is rather complex, and dependent on the mass ratio M_r and the tension in the pipe, $\bar{T}$. For simplicity, we will describe this motion for $\bar{T} = 0$. For $u_0 = 0$, the eigenvalues are at $\{\pm i\pi^2, \pm 4i\pi^2\}$. As u_0 is increased, both pairs of eigenvalues move towards the origin along the imaginary axis, until $u_0 = \pi$, when the eigenvalues from the first mode become zero. These eigenvalues split, and move onto the real axis. Eventually, this first mode pair of eigenvalues reverses its direction, and moves back towards the origin. What happens next depends on the value of M_r. If $M_r < (3\sqrt{3}/32)\pi$, then the eigenvalues from the second mode reach zero at $u_0 = 2\pi$, split, and move onto the real axis. These eigenvalues eventually coalesce along the real axis, and leave that axis. For $M_r > (3\sqrt{3}/32)\pi$, the eigenvalues from the first mode reach zero first at $u_0 = 2\pi$, restabilizing that mode. The two pairs of eigenvalues eventually coalesce along the imaginary axis, and split, indicating the onset of flutter. These two cases are shown in Fig. 1. In this figure, the eigenvalues are slightly displaced from the axes for clarity. The first mode is shown as a solid line, and the second mode is shown as a dashed line.

Thus, there are two critical flow velocities at which the system has a double zero eigenvalue, $u_0 = \pi$ and $u_0 = 2\pi$. If tension is present in the system, the corresponding critical flow velocities are $u_0 = (\pi^2 + \bar{T})^{1/2}$ and $u_0 = (4\pi^2 + \bar{T})^{1/2}$. A key idea here is that as the flow velocity u_0 increases from zero, both pairs of eigenvalues approach the origin initially. In this research, we vary the flow rate u_0 while maintaining a constant value of the tension $\bar{T}$ (often we set $\bar{T} = 0$ for simplicity). However, we could also analyze the effects of varying the tension, while keeping the flow rate constant, or varying both parameters simultaneously. In Fig. 2 we plot the two critical points, at which the system has a double zero eigenvalue, in the $\bar{T} - u_0$ plane. The shaded region A in this figure is stable. Part of the region C may also be stable as described above for the case $M_r > (3\sqrt{3}/32)\pi$. We can see from this figure that qualitatively, increasing the flow velocity u_0 is equivalent to decreasing the tension $\bar{T}$. We remark that at $M_r = (3\sqrt{3}/32)\pi$, the system possesses four zero eigenvalues, an interesting degenerate case.

The next step is to calculate the linear normal form for the system at these critical flow velocities. Since the generalized eigenspaces are symplectic, we can use the eigenvectors to generate the symplectic transformations. When $u_0 = (\pi^2 + \bar{T})^{1/2}$, the system has eigenvalues and kernel

$$0, 0, \pm i\sqrt{12\pi^4 + \tfrac{256}{9}M_r^2(\pi^2 + \bar{T})},$$

$$\ker A = \text{span}\left[1, 0, 0, \frac{8}{3}M_r\sqrt{\pi^2 + \bar{T}}\right] = \text{span}[1, 0, 0, \bar{\omega}_1],$$

whereas when $u_0 = \sqrt{4\pi^2 + \bar{T}}$, the system has eigenvalues and kernel

$$0, 0, \pm i\sqrt{3\pi^4 - \tfrac{256}{9}M_r^2(4\pi^2 + \bar{T})},$$

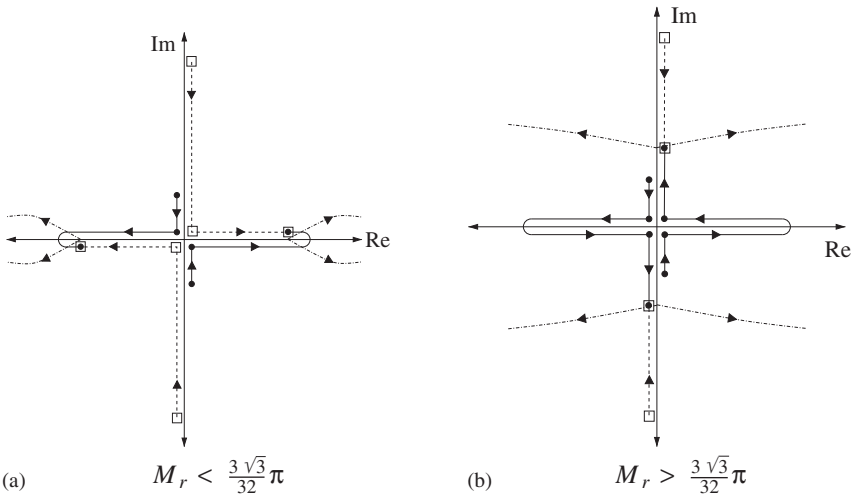

Fig. 1. Eigenvalue motion for pipe conveying fluid ($\bar{T} = 0$).

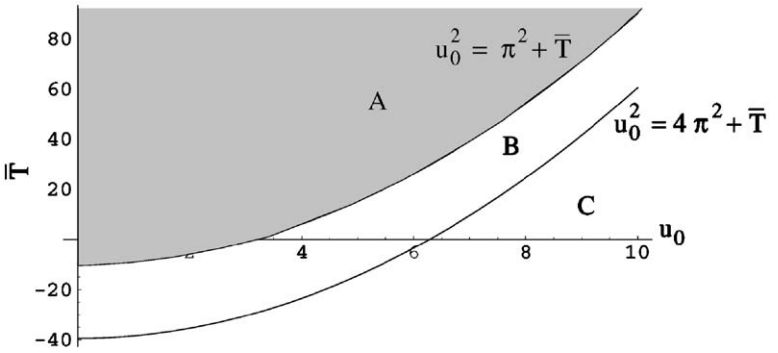

Fig. 2. Location of critical points in $\bar{T} - u_0$ parameter space.

$$\ker A = \text{span}\left[0, 1, -\tfrac{8}{3}M_r\sqrt{4\pi^2 + \bar{T}}, 0\right] = \text{span}[0, 1, -\bar{\omega}_2, 0].$$

Thus, we see that both double zero eigenvalue cases will correspond to nonsemisimple Jordan normal forms.

Next, we construct a transformation $\mathbf{x} = T\mathbf{z}$ that will put the linear system into normal form. To preserve the Hamiltonian structure, this transformation must be symplectic, i.e., it must satisfy the relation $T^{\mathrm{T}}JT = \mu J$. For simplicity, we will only proceed for the case $u_0 = (\pi^2 + \bar{T})^{1/2}$, that is, the point at which the pipe first becomes unstable through a divergence bifurcation. The second critical flow velocity, $u_0 = (4\pi^2 + \bar{T})^{1/2}$, may correspond to a restabilization of the first mode, or an instability in the second mode. Henceforth, all calculations will be assumed to be for the case $u_0 = (\pi^2 + \bar{T})^{1/2}$. We first calculate that at the critical flow velocity $u_0 = (\pi^2 + \bar{T})^{1/2}$

$$\bar{\omega}_1 = \tfrac{8}{3}Mr\sqrt{\pi^2 + \bar{T}}, \quad \bar{\omega}_2 = \sqrt{12\pi^4 + \tfrac{64}{9}M_r^2(\pi^2 + \bar{T})}$$

and thus, we define, for convenience

$$\bar{\omega}^2 \stackrel{\text{def}}{=} \bar{\omega}_1^2 + \bar{\omega}_2^2 = 12\pi^4 + \tfrac{128}{9}M_r^2(\pi^2 + \bar{T}), \quad \bar{\omega}_2^2 - \bar{\omega}_1^2 = 12\pi^4,$$
$$\Lambda_1^2 \stackrel{\text{def}}{=} 3\bar{\omega}_1^2 + \bar{\omega}_2^2 = 12\pi^4 + \tfrac{256}{9}M_r^2(\pi^2 + \bar{T}).$$

For $u_0 = (\pi^2 + \bar{T})^{1/2}$, the matrix T which transforms the system to a complex normal form is given by

$$T = [u_1 + \mathrm{i}v_1 \;\; u_2 + \mathrm{i}v_2 \;\; u_1 - \mathrm{i}v_1 \;\; u_2 - \mathrm{i}v_2], \tag{8}$$

where

$$u_1 = \begin{bmatrix} \dfrac{\sqrt{\bar{\omega}_2^2 - \bar{\omega}_1^2}}{\sqrt{2}\Lambda_1} \\ 0 \\ 0 \\ \dfrac{\sqrt{\bar{\omega}_2^2 - \bar{\omega}_1^2}\omega_1}{\sqrt{2}\Lambda_1} \end{bmatrix}, \quad v_1 = \begin{bmatrix} -\dfrac{\sqrt{\bar{\omega}_2^2 - \bar{\omega}_1^2}}{\sqrt{2}\Lambda_1} \\ \dfrac{\sqrt{2}\omega_1}{\sqrt{\bar{\omega}_2^2 - \bar{\omega}_1^2}\Lambda_1} \\ -\dfrac{\omega_1^2 + \omega_2^2}{\sqrt{2}\sqrt{\bar{\omega}_2^2 - \bar{\omega}_1^2}\Lambda_1} \\ -\dfrac{\sqrt{\bar{\omega}_2^2 - \bar{\omega}_1^2}\omega_1}{\sqrt{2}\Lambda_1} \end{bmatrix},$$

$$u_2 = \begin{bmatrix} \dfrac{\omega_1}{\Lambda_1^{\frac{3}{2}}} \\ -\dfrac{1}{2\sqrt{\Lambda_1}} \\ -\dfrac{\omega_1}{2\sqrt{\Lambda_1}} \\ -\dfrac{\omega_1^2 + \omega_2^2}{2\Lambda_1^{\frac{3}{2}}} \end{bmatrix}, \quad v_2 = \begin{bmatrix} -\dfrac{\omega_1}{\Lambda_1^{\frac{3}{2}}} \\ -\dfrac{1}{2\sqrt{\Lambda_1}} \\ -\dfrac{\omega_1}{2\sqrt{\Lambda_1}} \\ \dfrac{\omega_1^2+\omega_2^2}{2\Lambda_1^{\frac{3}{2}}} \end{bmatrix}.$$

This transformation is symplectic with multiplier $\mu = \frac{1}{\mathrm{i}}$, so that the new Hamiltonian is given by

$$K(\mathbf{z}) = \mu H(T\mathbf{z}) = -\mathrm{i}H(T\mathbf{z}) = \frac{\mathrm{i}}{4}(z_1 - \bar{z}_1)^2 - \mathrm{i}\Lambda_1 z_2 \bar{z}_2, \tag{9}$$

with corresponding linear matrix

$$\hat{A} = \begin{bmatrix} -\dfrac{\mathrm{i}}{2} & 0 & \dfrac{\mathrm{i}}{2} & 0 \\ 0 & -\mathrm{i}\Lambda_1 & 0 & 0 \\ -\dfrac{\mathrm{i}}{2} & 0 & \dfrac{\mathrm{i}}{2} & 0 \\ 0 & 0 & 0 & \mathrm{i}\Lambda_1 \end{bmatrix}.$$

This matrix $\hat{A}$ is the unperturbed linear normal form for the system at the critical point $u_0 = (\pi^2 + \bar{T})^{1/2}$.

3.3. Introduction of bifurcation and detuning parameters

The linear normal form we have calculated in the previous section is fine if the flow velocity u_0 is exactly at the critical flow velocity $u_0^c = (\pi^2 + \bar{T})^{1/2}$. However, in the real world, we would like to study the system when it is near the critical point, say $u_0 = u_0^c + \tilde{\delta}$. It is more convenient to define $\tilde{\delta} = (3/8M_r)\delta$, so that

$$\frac{8}{3}M_r u_0 = \frac{8}{3}M_r\left(u_0^c + \frac{3}{8M_r}\delta\right) = \frac{8}{3}M_r u_0^c + \delta,$$

and the matrix A becomes

$$A = \begin{bmatrix} 0 & \frac{8}{3}M_r u_0^c + \delta & 1 & 0 \\ -\frac{8}{3}M_r u_0^c - \delta & 0 & 0 & 1 \\ -\bar{\omega}_1^2 & 0 & 0 & \frac{8}{3}M_r u_0^c + \delta \\ 0 & -\bar{\omega}_2^2 & -\frac{8}{3}M_r u_0^c - \delta & 0 \end{bmatrix}. \tag{10}$$

We can break this matrix up into two components: one matrix at the critical point, and a second matrix which represents the perturbation from the critical case.

In this case, we find that

$$\bar{\omega}_{1,0} = \tfrac{8}{3} M_r \sqrt{\pi^2 + \bar{T}}, \quad \bar{\omega}_{2,0} = \sqrt{12\pi^4 + \tfrac{64}{9} M_r^2 (\pi^2 + \bar{T})},$$

where we have added the additional subscript 0 to denote that these expressions are calculated at the critical point, i.e., for $\delta = 0$. When the perturbation is added, we have

$$\bar{\omega}_1^2 = \bar{\omega}_{1,0}^2 + 2\tilde{\delta}\sqrt{\pi^2 + \bar{T}}\left(-\pi^2 + \tfrac{64}{9} M_r^2\right) + \mathcal{O}(\tilde{\delta}^2),$$
$$\bar{\omega}_2^2 = \bar{\omega}_{2,0}^2 + 2\tilde{\delta}\sqrt{\pi^2 + \bar{T}}\left(-4\pi^2 + \tfrac{64}{9} M_r^2\right) + \mathcal{O}(\tilde{\delta}^2).$$

Thus, the matrix A from (10) can be written as

$$A = A_0 + \delta A_1 + \mathcal{O}(\tilde{\delta}^2),$$

where

$$A_0 = \begin{bmatrix} 0 & \bar{\omega}_{1,0} & 1 & 0 \\ -\bar{\omega}_{1,0} & 0 & 0 & 1 \\ -\bar{\omega}_{1,0}^2 & 0 & 0 & \bar{\omega}_{1,0} \\ 0 & -\bar{\omega}_{2,0}^2 & -\bar{\omega}_{1,0} & 0 \end{bmatrix}$$

and

$$A_1 = \begin{bmatrix} 0 & 1 & 0 & 0 \\ -1 & 0 & 0 & 0 \\ -\dfrac{3}{4M_r}\sqrt{\pi^2 + \bar{T}}\left(\dfrac{64}{9} M_r^2 - \pi^2\right) & 0 & 0 & 1 \\ 0 & -\dfrac{3}{4M_r}\sqrt{\pi^2 + \bar{T}}\left(\dfrac{64}{9} M_r^2 - 4\pi^2\right) & -1 & 0 \end{bmatrix}.$$

Now we make the transformation T given in (8) to normalize A_0. The linear Hamiltonian of the system, including unfolding effects, is given by

$$H(\mathbf{x}, \delta) = \frac{1}{2}(p_1^2 + p_2^2) + \bar{\omega}_{1,0}(p_1 q_2 - p_2 q_1) + \frac{1}{2}(\bar{\omega}_{1,0}^2 q_1^2 + \bar{\omega}_{2,0}^2 q_2^2)$$
$$+ \delta\left((p_1 q_2 - p_2 q_1) + \frac{3}{8M_r}\sqrt{\pi^2 + \bar{T}}\left[\frac{64}{9} M_r^2 (q_1^2 + q_2^2) - \pi^2 (q_1^2 + 4q_2^2)\right]\right) + \mathcal{O}(\delta).$$

To determine the effect of the transformation T on the unfolding terms, we calculate

$$\hat{H}(\mathbf{z}, \delta) = \frac{1}{1} H(T\mathbf{z}, \delta).$$

As for the other terms in (3), we do not list the lengthy results of this calculation, instead waiting until we can determine which of these coefficients are important.

Before calculating the normal form for the pipe equations which we have developed, we want to detune the equations of motion. The purpose of this detuning is to allow us to understand what happens when the forcing frequency is near, but not necessarily at some critical forcing frequency. To detune the original equation, given in (3), we specify the form of the forcing as $f(t) = \cos \nu t$, where ν is the frequency of the input forcing. This choice explains the notation D_s and D_c, since those matrices multiply sin and cos functions, respectively. We thus introduce the detuning as $\nu = \omega_0(1 - \varepsilon\lambda)$, where λ is the small detuning parameter, and ω_0 is some critical frequency. We then rescale time by $\tau = \nu t$, and the equations of motion (3) become, with some simplification,

$$\omega_0 \mathbf{x}' = A_0 \mathbf{x} + JDH_1(\mathbf{x}) + \varepsilon(\delta A_1 + \lambda A_0 - h\omega_0 \sin\tau D_s + h\cos\tau D_c)\mathbf{x} - \varepsilon\zeta^{r*}(D_d \mathbf{x} + F(\mathbf{x})) + \mathcal{O}(\varepsilon^2), \tag{11}$$

where we have scaled $\delta \to \varepsilon\delta$ and the linear damping and forcing terms are given by

$$D_d = \begin{bmatrix} 0 & 0 & 0 & 0 \\ 0 & 0 & 0 & 0 \\ 0 & \omega_1\pi^4 & \pi^4 & 0 \\ -16\omega_1\pi^4 & 0 & 0 & 16\pi^4 \end{bmatrix}, \quad D_s = \begin{bmatrix} 0 & 0 & 0 & 0 \\ 0 & 0 & 0 & 0 \\ \dfrac{3\omega_1\pi^2}{16} & \dfrac{8\omega_1}{3} & 0 & 0 \\ \dfrac{2\omega_1}{3} & \dfrac{3\omega_1\pi^2}{4} & 0 & 0 \end{bmatrix}$$

and

$$D_c = \begin{bmatrix} 0 & 0 & 0 & 0 \\ 0 & 0 & 0 & 0 \\ \omega_1^2\left(\dfrac{9\pi^2}{32M_r^2} - 2\right) & 0 & 0 & 2\omega_1 \\ 0 & \omega_1^2\left(\dfrac{9\pi^2}{8M_r^2} - 2\right) & -2\omega_1 & 0 \end{bmatrix}.$$

The normal form of the system will be based on the form of the matrix A_0, which is nonsemisimple. Once again we use the transformation $\mathbf{x} = T\mathbf{z}$ defined in (8) that will put the linear system into normal form as before. The forcing terms can be separated into Hamiltonian terms and non-Hamiltonian terms. When we perform the normal form transformations for the pipe, we will see that only the Hamiltonian terms survive in the normal form.

4. Normal forms

In our analysis, we would like to reduce the original system to as simple a form as possible, that is, we want to find the simplest form of the nonlinear terms that captures the qualitative dynamics of the system. Ideally, we would like to make a series of coordinate transformations to completely eliminate all of the nonlinear terms. When the system we are studying is Hamiltonian, we also want the reduced system to be Hamiltonian. To achieve this, the normal form transformations should be symplectic.

4.1. Hamiltonian normal form

In this section, we calculate the normal form for the Hamiltonian function of the pipe. The Hamiltonian terms in the equations of motion include the following: the unperturbed linear matrix A_0, the δ-perturbations to A_0, the detuning terms, and the nonlinear Hamiltonian terms. So far, we have made a symplectic transformation to transform the unperturbed linear matrix to the form A_0. We also calculated the effect of this transformation on the rest of the terms. Next, we want to make a symplectic transformation to transform A_1 into its normal form.

The method of normal forms for autonomous Hamiltonian systems is described in Meyer and Hall (1992) and is also described briefly in Nagata and Namachchivaya (1998). We shall follow the algorithm for obtaining the normal form for a nonautonomous Hamiltonian system given in McDonald et al. (1999).

In the previous section, we found that the unperturbed Hamiltonian in the complex z coordinates is given by

$$H_0^0 = \frac{1}{\omega_0}\{\tfrac{1}{4}(z_1 - \bar{z}_1)^2 - \mathrm{i}\Lambda_1 z_2\bar{z}_2\}.$$

The basis for the normal form can be found as the kernel of the adjoint of the linear operator, $\ker D_{A^*}$, where D_A has been defined in McDonald et al. (1999) as

$$D_A^k = \{H_0^0, \cdot\} \quad D_A^k : \mathscr{H}_n^{k,2\pi} \longrightarrow \mathscr{H}_n^{k,2\pi},$$

where $\mathscr{H}_n^{k,2\pi}$ is the space of homogeneous polynomials of degree k in n variables, with 2π periodic coefficients which are C^∞ in t. We split this Hamiltonian, and its adjoint (the Hamiltonian associated with A^*) into semisimple and nilpotent parts

$$H_S = -\frac{\mathrm{i}\Lambda}{\omega_0} z_2 \bar{z}_2, \quad H_N = \frac{\mathrm{i}}{4\omega_0}(z_1 - \bar{z}_1)^2,$$

$$H_S^* = \frac{\mathrm{i}\Lambda}{\omega_0} z_2 \bar{z}_2, \quad H_N^* = \frac{\mathrm{i}}{4\omega_0}(z_1 + \bar{z}_1)^2.$$

The normal form must belong to the intersection of the kernel of the operators D_{S^*} and D_{N^*}, that is, $\ker D_{A^*} = \ker D_{S^*} \cap \ker D_{N^*}$, where the operators are given by

$$D_{S^*} = \frac{\mathrm{i}\Lambda}{\omega_0}\left(\bar{z}_2 \frac{\partial}{\partial \bar{z}_2} - z_2 \frac{\partial}{\partial z_2}\right) + \frac{\partial}{\partial t}, \quad D_{N^*} = \frac{\mathrm{i}}{2\omega_0}(z_1 + \bar{z}_1)\left(\frac{\partial}{\partial \bar{z}_1} - \frac{\partial}{\partial z_1}\right).$$

For terms of the form $z_1^{m_1} z_2^{m_2} \bar{z}_1^{m_3} \bar{z}_2^{m_4} \mathrm{e}^{\mathrm{i}st}$ the condition to be in the kernel of D_{S^*} is $s = \Lambda(m_2 - m_4)$. We then calculate the action of the operator D_{N^*} on terms in $\ker D_{S^*}$ [see McDonald et al. (1999) for the details of this calculation]. Then, by calculating the matrix representation of the action of D_{N^*} on $\ker D_{S^*}$, and finding the kernel of this matrix, we can determine the normal form. Thus, the Hamiltonian normal form, including unfolding and nonlinearities, is given by

$$H(\mathbf{z}) = \frac{1}{\omega_0}\left\{\frac{\mathrm{i}}{4}(z_1 - \bar{z}_1)^2 + \frac{\mathrm{i}\beta_1\delta}{4}(z_1 + \bar{z}_1)^2 - \mathrm{i}(\Lambda_1 - \beta_2\delta) z_2\bar{z}_2 + \mathrm{i}\alpha_1(z_1 + \bar{z}_1)^4 + \mathrm{i}\alpha_2(z_1 + \bar{z}_1)^2 z_2\bar{z}_2 + \mathrm{i}\alpha_3 z_2^2\bar{z}_2^2\right\},$$

where we can determine the coefficients of the nonlinear terms as

$$\alpha_1 = -\frac{9\kappa\pi^{12}}{\Lambda_1^4}, \quad \alpha_2 = -\frac{12\kappa\pi^8(\Lambda_1^2 + 3\omega_1^2)}{\Lambda_1^5}, \quad \alpha_3 = -\frac{2\kappa\pi^4(3\Lambda_1^4 + 2\Lambda_1^2\omega_1^2 + 3\omega_1^4)}{\Lambda_1^6}$$

and the coefficients of the autonomous unfolding terms as

$$\beta_1 = \frac{27\pi^6\omega_1}{8M_r^2\Lambda_1^2}, \quad \beta_2 = \frac{\omega_1(\Lambda_1^2(9\pi^2 - 64M_r^2) + 9\pi^2\omega_1^2)}{16M_r^2\Lambda_1^3}.$$

Since the physical parameter $\kappa = AL^2/2I$, we can see that each of the coefficients α_1, α_2, and α_3 are negative. It is obvious that $\beta_1 > 0$. And observing that $9\pi^2 - 64M_r^2 > 0$ for $M_r \in (0, 1)$, we can show that $\beta_2 > 0$.

4.2. Normal form for damping and forcing terms

The next step in the analysis is to determine the normal form for the damping and forcing terms. We find the following basis for the normal form for the linear damping and forcing terms:

$$\text{damping:} \quad \delta_1 \begin{bmatrix} z_1 \\ 0 \\ \bar{z}_1 \\ 0 \end{bmatrix} + \delta_2 \begin{bmatrix} 0 \\ z_2 \\ 0 \\ 0 \end{bmatrix} + \delta_3 \begin{bmatrix} z_1 + \bar{z}_1 \\ 0 \\ -(z_1 + \bar{z}_1) \\ 0 \end{bmatrix} + \delta_4 \begin{bmatrix} 0 \\ 0 \\ 0 \\ \bar{z}_2 \end{bmatrix},$$

$$\text{forcing:} \quad \sigma_1 \begin{bmatrix} z_2 \mathrm{e}^{\mathrm{i}\frac{\Lambda_1}{\omega_0}\tau} \\ 0 \\ -z_2 \mathrm{e}^{\mathrm{i}\frac{\Lambda_1}{\omega_0}\tau} \\ 0 \end{bmatrix} + \sigma_2 \begin{bmatrix} \bar{z}_2 \mathrm{e}^{-\mathrm{i}\frac{\Lambda_1}{\omega_0}\tau} \\ 0 \\ -\bar{z}_2 \mathrm{e}^{-\mathrm{i}\frac{\Lambda_1}{\omega_0}\tau} \\ 0 \end{bmatrix} + \sigma_3 \begin{bmatrix} 0 \\ (z_1 + \bar{z}_1)\mathrm{e}^{-\mathrm{i}\frac{\Lambda_1}{\omega_0}\tau} \\ 0 \\ 0 \end{bmatrix} + \sigma_4 \begin{bmatrix} 0 \\ \bar{z}_2 \mathrm{e}^{-2\mathrm{i}\frac{\Lambda_1}{\omega_0}\tau} \\ 0 \\ 0 \end{bmatrix}$$
$$+ \sigma_5 \begin{bmatrix} 0 \\ 0 \\ 0 \\ (z_1 + \bar{z}_1)\mathrm{e}^{\mathrm{i}\frac{\Lambda_1}{\omega_0}\tau} \end{bmatrix} + \sigma_6 \begin{bmatrix} 0 \\ 0 \\ 0 \\ z_2 \mathrm{e}^{2\mathrm{i}\frac{\Lambda_1}{\omega_0}\tau} \end{bmatrix}.$$

Using reality conditions, i.e., the second two equations are conjugates of the first two equations, we know that $\delta_4 = \bar{\delta}_2$, $\sigma_2 = -\bar{\sigma}_1$, $\sigma_5 = \bar{\sigma}_3$, and $\sigma_6 = \bar{\sigma}_4$. We can also determine that δ_1 must be real, while δ_3 must be imaginary. Thus, we have three independent damping coefficients to determine, and three forcing coefficients. We also note that the terms with coefficients σ_1, σ_2, σ_3, and σ_5 only occur for the combination resonance case, while the terms with coefficients σ_4

and σ_6 only occur for the subharmonic resonance case. The next step is to calculate the coefficients of these normal form terms.

Thus, we can find the damping coefficients in terms of the original coefficients as

$$\delta_1 = -\frac{6\zeta^*\pi^8}{\Lambda_1^2}, \quad \delta_2 = -\frac{2\zeta^*\pi^4(4\Lambda_1^2+\omega_1^2)}{\Lambda_1^2} = \bar{\delta}_2, \quad \delta_3 = 0$$

and the forcing coefficients

$$\sigma_1 = \frac{\varepsilon h\omega_1\pi^2(27\pi^2\omega_1^2(1+\mathrm{i}) + 32M_r^2\Lambda_1^2(1+\mathrm{i}) - 18M_r^2\pi^2\Lambda_1\omega_1(1-\mathrm{i}))}{32\sqrt{6}M_r^2\Lambda_1^{5/2}},$$

$$\sigma_3 = \frac{\varepsilon h\omega_1\pi^2(-27\pi^2\omega_1^2(1-\mathrm{i}) - 32M_r^2\Lambda_1^2(1-\mathrm{i}) + 18M_r^2\pi^2\Lambda_1\omega_1(1+\mathrm{i}))}{32\sqrt{6}M_r^2\Lambda_1^{5/2}},$$

$$\sigma_4 = \varepsilon h\omega_1^2\left(\frac{-320M_r^2\Lambda_1^2 + 27\pi^2(\Lambda_1^2-\omega_1^2)}{96M_r^2\Lambda_1^3} - \frac{3\mathrm{i}\pi^2(\Lambda_1^2-\omega_1^2)}{8\Lambda_1^2\omega_1}\right).$$

We see here that $\sigma_3 = -\bar{\sigma}_1$, so in fact, we only have two distinct forcing coefficients, σ_1 and σ_4. Also note that the forcing terms are now conservative, i.e., all of the nonconservative forcing terms were eliminated by the normal form procedure. Thus, the forcing terms can be simply represented as a Hamiltonian function:

$$\text{combination resonance:} \quad \sigma_1(z_1+\bar{z}_1)z_2\mathrm{e}^{\mathrm{i}\tau} - \bar{\sigma}_1(z_1+\bar{z}_1)\bar{z}_2\mathrm{e}^{-\mathrm{i}\tau},$$

$$\text{subharmonic resonance:} \quad -\frac{\sigma_4}{2}(z_2^2\mathrm{e}^{\mathrm{i}\tau} - \bar{z}_2^2\mathrm{e}^{-\mathrm{i}\tau}).$$

Note that the nonlinear Hamiltonian terms in the normal form have already been calculated by the Hamiltonian normal form procedure. Finally, the normal form for the nonlinear damping terms is given by

$$\phi_1\begin{bmatrix} z_1z_2\bar{z}_2 \\ 0 \\ \bar{z}_1z_2\bar{z}_2 \\ 0 \end{bmatrix} + \phi_2\begin{bmatrix} z_1(z_1+\bar{z}_1)^2 \\ 0 \\ \bar{z}_1(z_1+\bar{z}_1)^2 \\ 0 \end{bmatrix} + \phi_3\begin{bmatrix} (z_1+\bar{z}_1)z_2\bar{z}_2 \\ 0 \\ -(z_1+\bar{z}_1)z_2\bar{z}_2 \\ 0 \end{bmatrix} + \phi_4\begin{bmatrix} (z_1+\bar{z}_1)^3 \\ 0 \\ -(z_1+\bar{z}_1)^3 \\ 0 \end{bmatrix}$$
$$+ \phi_5\begin{bmatrix} 0 \\ z_2^2\bar{z}_2 \\ 0 \\ 0 \end{bmatrix} + \phi_6\begin{bmatrix} 0 \\ (z_1+\bar{z}_1)^2z_2 \\ 0 \\ 0 \end{bmatrix} + \phi_7\begin{bmatrix} 0 \\ 0 \\ 0 \\ z_2\bar{z}_2^2 \end{bmatrix} + \phi_8\begin{bmatrix} 0 \\ 0 \\ 0 \\ (z_1+\bar{z}_1)^2\bar{z}_2 \end{bmatrix}.$$

Using reality conditions, we can see that ϕ_1 and ϕ_2 must be real, ϕ_3 and ϕ_4 must be imaginary, $\phi_7 = \bar{\phi}_5$, and $\phi_8 = \bar{\phi}_6$.

The coefficients ϕ_i have contributions from three sources. First, we have contributions from the original nonlinear damping terms in our equations. Next, we have terms that are due to the action of transformations to normalize the linear damping terms on nonlinear Hamiltonian terms. Finally, we have terms due to the action of transformations to normalize the nonlinear Hamiltonian terms, acting on linear damping terms. These coefficients are combined and listed below

$$\phi_1 = -\frac{16\varepsilon\zeta^*\kappa\pi^4\omega_1^2(2\Lambda_1^2+3\pi^4)}{\Lambda_1^5} - \frac{16\varepsilon\zeta^*\kappa\pi^8\omega_1^2(13\Lambda_1^4+27\Lambda_1^2\omega_1^2+12\omega_1^4)}{\Lambda_1^9},$$

$$\phi_2 = -\frac{36\varepsilon\zeta^*\kappa\pi^{12}}{\Lambda_1^4} - \frac{12\varepsilon\zeta^*\kappa\pi^{12}\omega_1^2(23\Lambda_1^2+12\omega_1^2)}{\Lambda_1^8},$$

$$\phi_3 = -\frac{96\varepsilon\zeta^*\mathrm{i}\pi^{12}\kappa(78\omega_1^4+37\omega_1^2\omega_2^2+4\omega_2^4)}{\Lambda_1^7},$$

$$\phi_4 = \frac{864\varepsilon\zeta^*\mathrm{i}\pi^{20}\kappa}{\Lambda_1^6},$$

$$\phi_5 = -\frac{8\varepsilon\zeta^*\kappa\pi^4(\Lambda_1^2-\omega_1^2)^2}{\Lambda_1^5}+\frac{8\varepsilon\zeta^*\kappa\pi^8\omega_1^2(13\Lambda_1^4+27\Lambda_1^2\omega_1^2+12\omega_1^4)}{\Lambda_1^9},$$
$$\phi_6 = -\frac{24\varepsilon\zeta^*\kappa\pi^8\omega_1^2}{\Lambda_1^4}+\frac{24\varepsilon\zeta^*\kappa\pi^{12}\omega_1^2(23\Lambda_1^2+12\omega_1^2)}{\Lambda_1^8}+\frac{144\mathrm{i}\varepsilon\zeta^*\kappa\pi^{16}(6\omega_1^2+\omega_2^2)}{\Lambda_1^7},$$
$$\phi_7 = -\frac{8\varepsilon\zeta^*\kappa\pi^4(\Lambda_1^2-\omega_1^2)^2}{\Lambda_1^5}+\frac{8\varepsilon\zeta^*\kappa\pi^8\omega_1^2(13\Lambda_1^4+27\Lambda_1^2\omega_1^2+12\omega_1^4)}{\Lambda_1^9},$$
$$\phi_8 = -\frac{24\varepsilon\zeta^*\kappa\pi^8\omega_1^2}{\Lambda_1^4}+\frac{24\varepsilon\zeta^*\kappa\pi^{12}\omega_1^2(23\Lambda_1^2+12\omega_1^2)}{\Lambda_1^8}+\frac{144\mathrm{i}\varepsilon\zeta^*\kappa\pi^{16}(6\omega_1^2+\omega_2^2)}{\Lambda_1^7}.$$

We note that none of the coefficients are zero, and thus there are no degeneracies due to missing terms in the nonlinear damping. Looking at each of these terms, we see that ϕ_1 and ϕ_2 are both real (as expected), ϕ_3 and ϕ_4 are both imaginary (as expected), $\phi_5=\phi_7$ are real, and $\phi_6=\phi_8$ are complex.

4.3. Final equations of motion for pipe

Now that we have completed the exhaustive normal form calculations, we can write down the equations of motion in a simpler form. We have

$$\omega_0\dot{\mathbf{z}} = A_0\mathbf{z}+A_\lambda\mathbf{z}+\delta A_1\mathbf{z}+JDH_1(\mathbf{z})+P(t)\mathbf{z}+\zeta^*B\mathbf{z}+\zeta^*F(\mathbf{z}),$$

where

$$A_0=\begin{bmatrix}-\frac{\mathrm{i}}{2} & 0 & \frac{\mathrm{i}}{2} & 0\\ 0 & -\mathrm{i}\Lambda_1 & 0 & 0\\ -\frac{\mathrm{i}}{2} & 0 & \frac{\mathrm{i}}{2} & 0\\ 0 & 0 & 0 & \mathrm{i}\Lambda_1\end{bmatrix},\quad A_1=\begin{bmatrix}\frac{\mathrm{i}\beta_1}{2} & 0 & \frac{\mathrm{i}\beta_1}{2} & 0\\ 0 & \mathrm{i}\beta_2 & 0 & 0\\ -\frac{\mathrm{i}\beta_1}{2} & 0 & -\frac{\mathrm{i}\beta_1}{2} & 0\\ 0 & 0 & 0 & -\mathrm{i}\beta_2\end{bmatrix},$$

$$A_\lambda=\begin{bmatrix}0 & 0 & 0 & 0\\ 0 & -\mathrm{i}\Lambda_1 & 0 & 0\\ 0 & 0 & 0 & 0\\ 0 & 0 & 0 & \mathrm{i}\Lambda_1\end{bmatrix},\quad B=\begin{bmatrix}\delta_1 & 0 & 0 & 0\\ 0 & \delta_2 & 0 & 0\\ 0 & 0 & \delta_1 & 0\\ 0 & 0 & 0 & \delta_2\end{bmatrix},$$

$$P(t)=\begin{bmatrix}\sigma_1 z_2\mathrm{e}^{\mathrm{i}\frac{\Lambda_1}{\omega_0}t}-\bar{\sigma}_1\bar{z}_2\mathrm{e}^{-\mathrm{i}\frac{\Lambda_1}{\omega_0}t}\\ -\overline{\sigma}_1(z_1+\bar{z}_1)\mathrm{e}^{-\mathrm{i}\frac{\Lambda_1}{\omega_0}t}+\sigma_4\bar{z}_2\mathrm{e}^{-2\mathrm{i}\frac{\Lambda_1}{\omega_0}t}\\ -\sigma_1 z_2\mathrm{e}^{\mathrm{i}\frac{\Lambda_1}{\omega_0}t}+\bar{\sigma}_1\bar{z}_2\mathrm{e}^{-\mathrm{i}\frac{\Lambda_1}{\omega_0}t}\\ -\sigma_1(z_1+\bar{z}_1)\mathrm{e}^{\mathrm{i}\frac{\Lambda_1}{\omega_0}t}+\bar{\sigma}_4 z_2\mathrm{e}^{2\mathrm{i}\frac{\Lambda_1}{\omega_0}t}\end{bmatrix},$$

$$JDH_1(\mathbf{z})=\begin{bmatrix}4\mathrm{i}\alpha_1(z_1+\bar{z}_1)^3+2\mathrm{i}\alpha_2(z_1+\bar{z}_1)z_2\bar{z}_2\\ \mathrm{i}\alpha_2(z_1+\bar{z}_1)^2z_2+2\mathrm{i}\alpha_3z_2^2\bar{z}_2\\ -4\mathrm{i}\alpha_1(z_1+\bar{z}_1)^3-2\mathrm{i}\alpha_2(z_1+\bar{z}_1)z_2\bar{z}_2\\ -\mathrm{i}\alpha_2(z_1+\bar{z}_1)^2\bar{z}_2-2\mathrm{i}\alpha_3z_2\bar{z}_2^2\end{bmatrix},$$

$$F(\mathbf{z})=\begin{bmatrix}\phi_1z_1z_2\bar{z}_2+\phi_2z_1(z_1+\bar{z}_1)^2+\phi_3(z_1+\bar{z}_1)z_2\bar{z}_2+\phi_4(z_1+\bar{z}_1)^3\\ \phi_5z_2^2\bar{z}_2+\phi_6(z_1+\bar{z}_1)^2z_2\\ \phi_1\bar{z}_1z_2\bar{z}_2+\phi_2\bar{z}_1(z_1+\bar{z}_1)^2-\phi_3(z_1+\bar{z}_1)z_2\bar{z}_2-\phi_4(z_1+\bar{z}_1)^3\\ \phi_5z_2\bar{z}_2^2+\bar{\phi}_6(z_1+\bar{z}_1)^2\bar{z}_2\end{bmatrix}.$$

These equations are different from those obtained by Namachchivaya (1989) and Namachchivaya and Tien (1989a, b) for gyroscopic systems far from critical points. We also note that there are two critical cases where the forcing terms occur. At $\omega_0=\Lambda_1$, there is a combination resonance, and only the forcing terms with coefficients σ_1 are present, and at

$\omega_0 = 2\Lambda_1$, there is a subharmonic resonance, and only the forcing terms with coefficients σ_4 are present. When the system is near neither of these resonance frequencies, none of the forcing terms are present. Thus, we have separate sets of equations for the two cases. We can further simplify these two cases by making a time-dependent symplectic transformation which eliminates the explicit time-dependence of the forcing terms. This transformation is given by

$$z_1 = w_1 \quad \bar{z}_1 = \bar{w}_1 \quad z_2 = w_2 e^{-(i\omega_0\tau/\Lambda_1)} \quad \bar{z}_2 = \bar{w}_2 e^{(i\omega_0\tau/\Lambda_1)}.$$

This transformation also removes the $\mathcal{O}(1)$ linear term from the second modal equation. Finally, we can scale time as $t = \omega_0\tau$ to eliminate the factor of $1/\Lambda_1$ or $1/2\Lambda_1$ in each of the equations. Thus, we have

$$\begin{aligned}
\dot{w}_1 = & -\frac{i}{2}(w_1 - \bar{w}_1) + \frac{i\beta_1\delta}{2}(w_1 + \bar{w}_1) + 4i\alpha_1(w_1 + \bar{w}_1)^3 + 2i\alpha_2(w_1 + \bar{w}_1)w_2\bar{w}_2 + \zeta^*\delta_1 w_1 + \sigma_1 w_2 - \bar{\sigma}_1\bar{w}_2 \\
& + \zeta^*[\phi_1 w_1 w_2\bar{w}_2 + \phi_2 w_1(w_1 + \bar{w}_1)^2 + \phi_3(w_1 + \bar{w}_1)w_2\bar{w}_2 + \phi_4(w_1 + \bar{w}_1)^3], \\
\dot{w}_2 = & -i\lambda\Lambda_1 w_2 + i\beta_2\delta w_2 + i\alpha_2(w_1 + \bar{w}_1)^2 w_2 + 2i\alpha_3 w_2^2\bar{w}_2 + \zeta^*\delta_2 w_2 - \bar{\sigma}_1(w_1 + \bar{w}_1) + \sigma_4\bar{w}_2 \\
& + \zeta^*[\phi_5 w_2^2\bar{w}_2 + \phi_6(w_1 + \bar{w}_1)^2 w_2].
\end{aligned} \tag{12}$$

We note that the equations for the two cases (subharmonic and combination resonances) are now identical, except for the forcing terms.

As calculated earlier, the unperturbed Hamiltonian is the same regardless of the forcing, and is given by

$$\begin{aligned}
H = & \frac{i}{4}(w_1 - \bar{w}_1)^2 + \frac{i\beta_1\delta}{4}(w_1 + \bar{w}_1)^2 - i\Lambda_1(1 + \lambda)w_2\bar{w}_2 + i\beta_2\delta w_2\bar{w}_2 \\
& + i\alpha_1(w_1 + \bar{w}_1)^4 + i\alpha_2(w_1 + \bar{w}_1)^2 w_2\bar{w}_2 + i\alpha_3 w_2^2\bar{w}_2^2.
\end{aligned}$$

5. Local bifurcation close to subharmonic resonance case

In this section, we study the local dynamics of pipes conveying pulsating fluid close to the subharmonic resonance. The rectangular form for the equations of motion (12) is

$$\begin{aligned}
\dot{x}_1 &= \beta_1\delta y_1 + 32\alpha_1 y_1^3 + 4\alpha_2(x_2^2 + y_2^2)y_1 + \zeta\delta_1 x_1 + \zeta(\phi_1 x_1(x_2^2 + y_2^2) + 4\phi_2 x_1 y_1^2 + 2\phi_3 y_1(x_2^2 + y_2^2) + 8\phi_4 y_1^3), \\
\dot{y}_1 &= x_1 + \zeta\delta_1 y_1 + \zeta(\phi_1 y_1(x_2^2 + y_2^2) + 4\phi_2 y_1^3), \\
\dot{x}_2 &= -\sigma_4^r x_2 + \sigma_4^i y_2 + (\beta_2\delta - \Lambda_1)y_2 + \delta_2 x_2 + 4\alpha_2 y_1^2 y_2 + 2\alpha_3 y_2(x_2^2 + y_2^2) + \zeta(\phi_5 x_2(x_2^2 + y_2^2) + 4\phi_6^r x_2 y_1^2 + 4\phi_6^i y_2 y_1^2), \\
\dot{y}_2 &= +\sigma_4^r y_2 + \sigma_4^i x_2 - (\beta_2\delta - \Lambda_1)x_2 + \delta_2 y_2 - 4\alpha_2 y_1^2 x_2 - 2\alpha_3 x_2(x_2^2 + y_2^2) + \zeta(\phi_5 y_2(x_2^2 + y_2^2) \\
&\quad + 4\phi_6^r y_2 y_1^2 - 4\phi_6^i x_2 y_1^2),
\end{aligned} \tag{13}$$

where the superscripts r and i denote the real and imaginary parts of the parameters that are defined in Section 4.2.

5.1. Nonlinear damped system

In this section, we only consider the effects of nonlinear damping to the unforced system. The rectangular form for the equations of motion is the same as (13) with $\sigma_4^r = 0$ and $\sigma_4^i = 0$. The trivial solution becomes unstable at one point, given by $\delta = \zeta^2\delta_1^2/\beta_1$. At this point, we expect a bifurcation to occur into the plane of the first mode. However, as we shall see below, the nonlinear damping will affect the form of the bifurcating solutions, and the types of bifurcations that are possible on those solutions.

5.1.1. Single mode solutions

We look for first-mode solutions with $x_2 = y_2 = 0$. We find two real solutions in $x_1 - y_1$ coordinates, corresponding to one branch in action-angle coordinates $I_1 = (x_1^2 + y_1^2)/2$. This solution is

$$I_1^a = \frac{(4\alpha_1 - \delta_1\zeta\phi_2 + \zeta\phi_4 + \sqrt{E})(\zeta^2\phi_2^2 + (4\alpha_1 + \zeta\phi_4 + \sqrt{E})^2)}{8\zeta^4\phi_2^4}, \tag{14}$$

$$E = (4\alpha_1 - \zeta^2\delta_1\phi_2 + \zeta\phi_4)^2 + (\beta_1\delta - \zeta^2\delta_1^2)\zeta^2\phi_2^2.$$

In order for this solution to exist, we must have $I_1 > 0$, i.e.,

$$I_1^a \text{ exists if:} \quad 4\alpha_1 - \zeta^2\delta_1\phi_2 + \zeta\phi_4 + \sqrt{E} > 0. \tag{15}$$

After some simplification, we find that (15) is satisfied if $\delta > \zeta^2\delta_1^2/\beta_1$. Therefore, the solution branch I_1^a exists for $\delta > \zeta^2\delta_1^2/\beta_1$. This branch in action-angle coordinates represents two branches in (x_1, y_1) coordinates. We also know that this branch is supercritical.

Next, we can examine the stability of the first-mode branch by evaluating the Jacobian of the system along the bifurcation branch I_1^a. We can show that I_1^a may undergo a simple bifurcation into the plane of the first mode at

$$\delta_{S_1} = \frac{-16\alpha_1^2 + 8\zeta^2\alpha_1\delta_1\phi_2 - 8\zeta\alpha_1\phi_4 + 2\zeta^3\delta_1\phi_2\phi_4 - \zeta^2\phi_4^2}{\zeta^2\beta_1\phi_2^2}.$$

Assuming that $\zeta \ll 1$, this point would occur near $\delta_{S_1} \approx -16\alpha_1^2/\zeta^2\beta_1\phi_2^2 < 0$, at which point I_1^a does not exist, so there is no simple bifurcation into the plane of the first mode. We can also determine that I_1^a may go through a Hopf bifurcation into the I_1 plane at

$$\delta_{H_1} = \frac{\delta_1^2}{4\beta_1} + \frac{\delta_1(4\alpha_1 + \phi_4)}{\beta_1\phi_2}$$

as long as $\delta_{H_1} > \zeta^2\delta_1^2/\beta_1$. Also, I_1^a may undergo a Hopf bifurcation into the I_2 plane at

$$\delta_{H_2} = \frac{\zeta^2\delta_1^2}{\beta_1} + \frac{\zeta^2\delta_2^2\phi_2^2}{\beta_1(\phi_6^r)^2} + \frac{2\delta_2(4\alpha_1 - \zeta^2\delta_1\phi_2 + \zeta\phi_4)}{\beta_1\phi_6^r}$$

as long as $\delta_{H_2} > \zeta^2\delta_1^2/\beta_1$. The condition for the solution to go through a simple bifurcation into the plane of the second mode is much more complicated, but can be evaluated numerically. We can easily show that there are no multi-mode solutions for the system. This fact would indicate that simple bifurcations do not occur to the plane of the second mode. Thus, the only bifurcations that the first-mode solutions may have are Hopf bifurcations.

Since the equations with nonlinear damping are difficult to examine analytically, we plot the bifurcations for this system numerically for a few cases, using the numerical bifurcation analysis software AUTO97 (Doedel et al., 1997). Plots for the case $M_r = 0.7$, $\bar{T} = 0$, $\zeta^* = 0.01$, $\kappa = 2$, $\sigma = 0.01$, $h = 0.0$, and $\lambda = 0.0$ are given in Figs. 3 and 4. In these figures, stable solutions are shown with solid lines, unstable solutions with dotted lines, simple (pitchfork) bifurcations are indicated by empty boxes, Hopf bifurcations by solid boxes, and periodic solutions by solid circles. The second-mode solutions do not exist for the unforced case. However, when nonlinear damping is present, a Hopf bifurcation

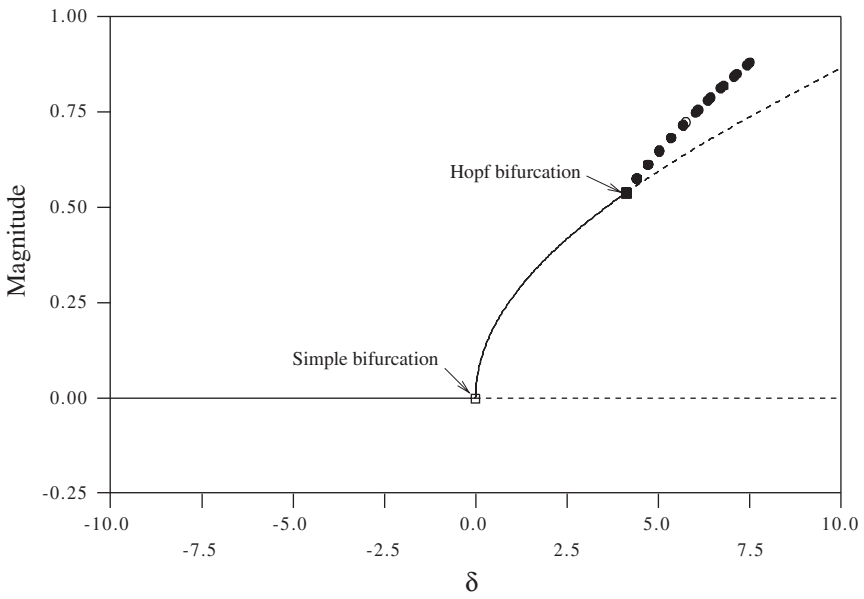

Fig. 3. Magnitude of response versus δ for $M_r = 0.7$, $\bar{T} = 0$, $\zeta^* = 0.01$, $\kappa = 2$, $\sigma = 0.01$, $h = 0.0$, and $\lambda = 0.0$.

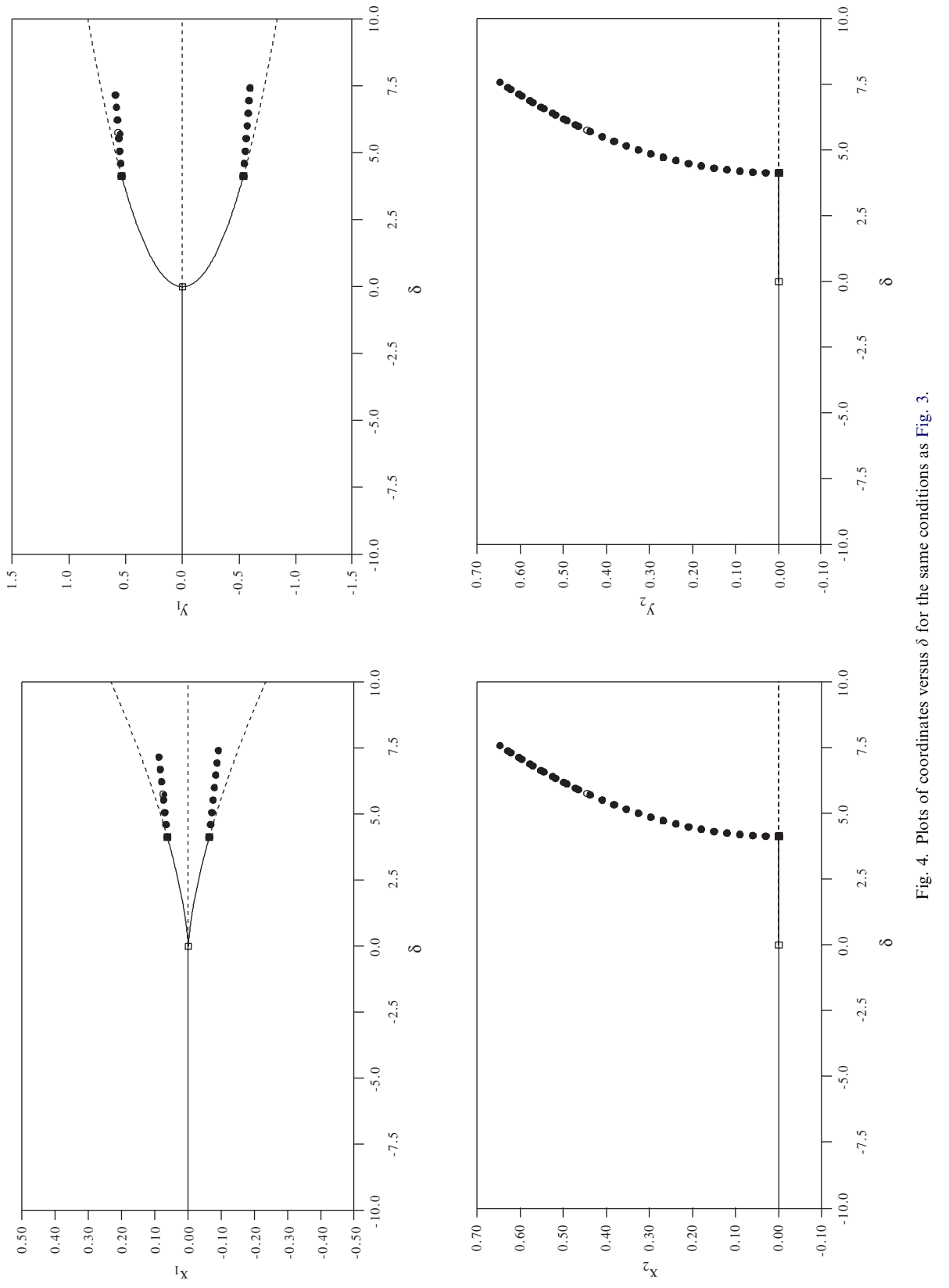

Fig. 4. Plots of coordinates versus δ for the same conditions as Fig. 3.

may be present, leading to solutions which have a constant component in the first mode, but a periodic component in the second mode. Plots for the case $M_r = 0.7$, $\bar{T} = 0$, $\zeta^* = 0.01$, $\kappa = 2$, $\sigma = 0.1$, $h = 0.0$, and $\lambda = 0.0$ are given in Figs. 5 and 6. In this case, the first-mode solution does not go through a Hopf bifurcation, but remains always stable. The plots of x_2 and y_2 are not shown, since these coordinates are always zero due to the lack of any steady state or periodic solutions with components in the second mode. We can now draw a few conclusions about the unforced equations with damping. First, the trivial solution only undergoes one bifurcation, a simple bifurcation at $\delta = \zeta^2\delta_1^2/\beta_1$, which is very near to zero for $\zeta \ll 1$. This bifurcation leads to a new, supercritical branch of solutions (actually two branches in the $x_1 - y_1$ coordinates). This branch is initially stable, but may undergo a Hopf bifurcation if nonlinear damping is present. If no nonlinear damping is present, this branch is always stable. Also, there are no second-mode solution branches or multi-mode solution branches. The presence of first-mode branches is expected, since we have set our problem up so that the first mode becomes unstable. Also, we expected that there would be no second-mode branches in the absence of forcing, since the eigenvalues corresponding to the second mode are far from zero. For the rest of this paper, we include the effects of forcing in our analysis.

5.2. Undamped, forced system

Now, we look at the forced system with no damping, either linear or nonlinear. In the subharmonic case, the forcing only enters into the equations off motion in the second mode. The equations of motion are then given by

$$\begin{aligned}
\dot{x}_1 &= \beta_1\delta y_1 + 32\alpha_1 y_1^3 + 4\alpha_2 y_1(x_2^2 + y_2^2),\\
\dot{y}_1 &= x_1,\\
\dot{x}_2 &= (\beta_2\delta - \lambda\Lambda_1)y_2 + 4\alpha_2 y_1^2 y_2 + 2\alpha_3 y_2(x_2^2 + y_2^2) - \sigma_4^r x_2 + \sigma_4^i y_2,\\
\dot{y}_2 &= -(\beta_2\delta - \lambda\Lambda_1)x_2 - 4\alpha_2 y_1^2 x_2 - 2\alpha_3 x_2(x_2^2 + y_2^2) + \sigma_4^r y_2 + \sigma_4^i x_2.
\end{aligned} \tag{16}$$

Note that for the pipe system $\sigma_4^r \neq 0$ and $\sigma_4^i \neq 0$.

The eigenvalues of (16), linearized about the trivial solution, are

$$\lambda_{1,2} = \pm\sqrt{\beta_1\delta}, \quad \lambda_{3,4} = \pm i\sqrt{(\beta_2\delta - \lambda\Lambda_1)^2 - \sigma_4^2}.$$

For simplicity, we have defined

$$\sigma_4^2 \stackrel{\text{def}}{=} (\sigma_4^i)^2 + (\sigma_4^r)^2,$$

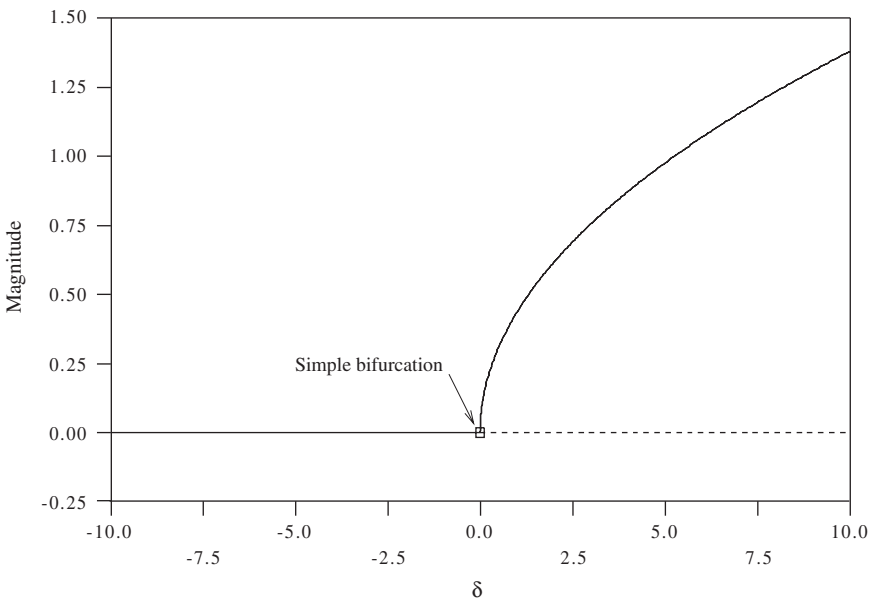

Fig. 5. Magnitude of response versus δ for $M_r = 0.7$, $\bar{T} = 0$, $\zeta^* = 0.01$, $\kappa = 2$, $\sigma = 0.1$, $h = 0.0$, and $\lambda = 0.0$.

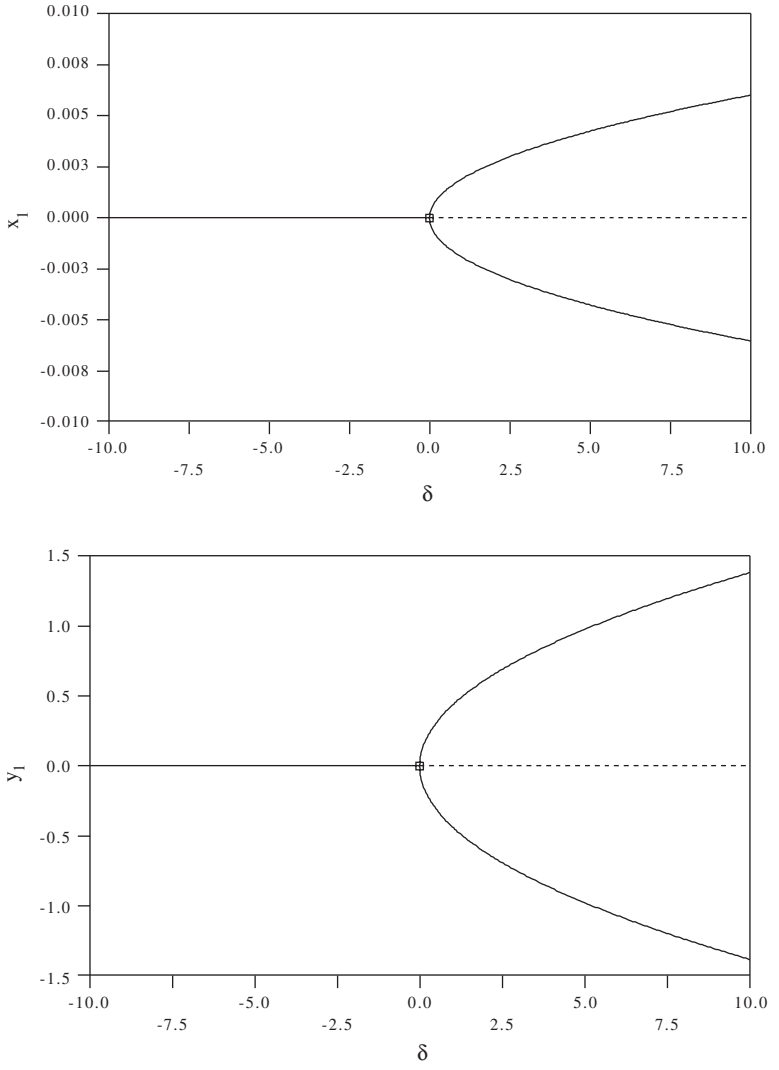

Fig. 6. Plots of coordinates versus δ for the same conditions as Fig. 5.

where $\sigma_4 > 0$. The first pair of eigenvalues is imaginary for $\delta < 0$, zero at $\delta = 0$, and real for $\delta > 0$. Thus, the system is unstable for $\delta > 0$. The second pair of eigenvalues behaves differently for ($\beta_2 < 0$) and ($\beta_2 > 0$). Since $\beta_2 > 0$ for the pipe, we will be interested in this scenario for the eigenvalues of the trivial solution:

$$\text{eigenvalues imaginary:} \quad \delta < \frac{\lambda\Lambda_1 - \sigma_4}{\beta_2} \quad \text{or} \quad \delta > \frac{\lambda\Lambda_1 + \sigma_4}{\beta_2};$$

$$\text{eigenvalues real:} \quad \frac{\lambda\Lambda_1 - \sigma_4}{\beta_2} < \delta < \frac{\lambda\Lambda_1 + \sigma_4}{\beta_2}.$$

Thus, we can determine the stability of the trivial solution as a function of δ and λ. This behavior is shown in Fig. 7, where the unshaded regions are stable, and the shaded regions are unstable. For a Hamiltonian system such as this, the eigenvalues are symmetric about the real and imaginary axes. Thus, the trivial solution is stable when all eigenvalues are on the imaginary axis, and unstable when at least one pair of eigenvalues is real.

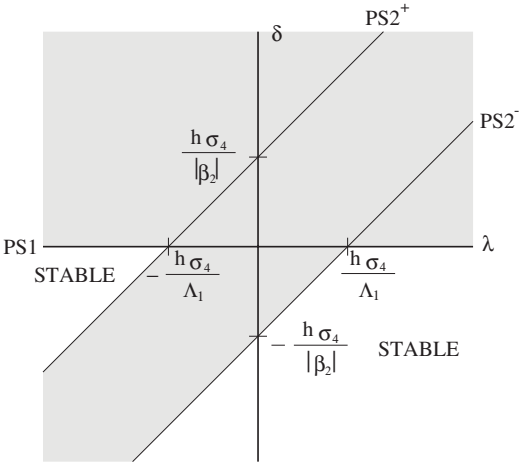

Fig. 7. Stability boundaries for trivial solution for undamped pipe.

5.2.1. First-mode solutions

Now we look for single-mode solutions to the nonlinear equations. We find a pair of first-mode solutions

$$PS1: \quad x_1 = 0, \quad y_1 = \pm\sqrt{-\frac{\beta_1\delta}{32\alpha_1}},$$

which we denote by $PS1$. As expected, these solutions only exist for $\delta > 0$ and are supercritical. We can determine that $PS1$ may have 0 , 1 , or 2 bifurcation points, given by

$$B_1: \quad \delta_{B_1} = \frac{8\alpha_1(-\lambda\Lambda_1 - \sigma_4)}{\alpha_2\beta_1 - 8\alpha_1\beta_2} \quad \text{and} \quad B_2: \quad \delta_{B_2} = \frac{8\alpha_1(-\lambda\Lambda_1 + \sigma_4)}{\alpha_2\beta_1 - 8\alpha_1\beta_2}.$$

We note that these bifurcations occur if the corresponding value of δ is greater than zero, and B_1 occurs for a lower value of δ than B_2. We know that $\alpha_1 < 0$, and we can show that the denominator $\alpha_2\beta_1 - 8\alpha_1\beta_2 < 0$ for the pipe. So we have the following existence criteria:

$$B_1 \text{ exists:} \quad \lambda < -\frac{\sigma_4}{\Lambda_1} \quad \text{and} \quad B_2 \text{ exists:} \quad \lambda < \frac{\sigma_4}{\Lambda_1}.$$

Furthermore, we can determine the following stability criteria for $PS1$ by examining the eigenvalues of the Jacobian of the system, linearized about $PS1$ yields

$$\text{stable for:} \quad -\frac{\sigma_4}{\Lambda_1} < \lambda < \frac{\sigma_4}{\Lambda_1} \quad \text{and} \quad \text{unstable for:} \quad \lambda < -\frac{\sigma_4}{\Lambda_1} \quad \text{or} \quad \lambda > \frac{\sigma_4}{\Lambda_1}.$$

Thus, for a fixed value of λ, we have three cases:

(i) for $\lambda > \sigma_4/\Lambda_1$, no bifurcation points exist on $PS1$, and the solution $PS1$ is always stable;
(ii) for $-\sigma_4/\Lambda_1 < \lambda < \sigma_4/\Lambda_1$, only B_2 exists, and the solution is unstable for $\delta < \delta_{B_2}$, and stable for $\delta > \delta_{B_2}$;
(iii) for $\lambda < -\sigma_4/\Lambda_1$, both bifurcations B_1 and B_2 exist, and the solution is unstable between the two bifurcations, and stable outside the two bifurcations.

5.2.2. Second-mode solutions

By setting $x_1 = y_1 = 0$, we can find second-mode solutions

$$x_2 = \pm\frac{(\sigma_4^i \pm \sigma_4)\sqrt{\beta_2\delta - \lambda\Lambda_1 + \sigma_4^i \pm [(\beta_2\delta - \lambda\Lambda_1)\sigma_4^i + \sigma_4^2]/\sigma_4}}{2\sqrt{-\alpha_3}\sigma_4^r},$$

$$y_2 = \pm\frac{1}{2}\sqrt{-\frac{\beta_2\delta - \lambda\Lambda_1 + \sigma_4^i \pm [(\beta_2\delta - \lambda\Lambda_1)\sigma_4^i + \sigma_4^2]/\sigma_4}{\alpha_3}}.$$

These solutions take an especially simple form in action-angle coordinates $I_2 = (x_2^2 + y_2^2)/2$, $\tan\theta_2 = x_2/y_2$:

$$PS2^-: \quad I_2 = \frac{\lambda\Lambda_1 - \beta_2\delta - \sigma_4}{4\alpha_3}, \quad \tan\theta_2 = \frac{\sigma_4^i - \sigma_4}{\sigma_4^r},$$

$$PS2^+: \quad I_2 = \frac{\lambda\Lambda_1 - \beta_2\delta + \sigma_4}{4\alpha_3}, \quad \tan\theta_2 = \frac{\sigma_4^i + \sigma_4}{\sigma_4^r}.$$

For the pipe, both of these solutions are supercritical, since the coefficient in front of δ, $-\beta_2/4\alpha_3$ is positive. These two solutions bifurcate from the trivial solution at

$$PS2^-: \quad \delta = \frac{\lambda\Lambda_1 - \sigma_4}{\beta_2} \quad \text{and} \quad PS2^+: \quad \delta = \frac{\lambda\Lambda_1 + \sigma_4}{\beta_2},$$

respectively and the bifurcation to $PS2^-$ occurs first.

A critical question to consider is whether the first-mode solution or the second-mode solutions bifurcate from the trivial solution first. The order in which these bifurcations occurs as δ is increased is summarized in Table 1. Fig. 7 shows not only the stability of the trivial solution, but where each of the bifurcations to modes $PS1$, $PS2^-$, and $PS2^+$ may occur.

Next, we can determine the stability of the second-mode solutions. First, we look at $PS2^-$. This branch may undergo a bifurcation at

$$B_3^-: \quad \delta_{B_3^-} = \frac{-2\alpha_2(\lambda\Lambda_1 - \sigma_4)}{\alpha_3\beta_1 - 2\alpha_2\beta_2}.$$

Of course, this bifurcation only occurs if $\delta_{B_3^-}$ is *greater than* the value at which the supercritical branch $PS2^-$ bifurcates from the trivial solution. The bifurcation point $\delta_{B_3^-}$ must occur for a positive value of I_2. We can show that $\alpha_3\beta_1 - 2\alpha_2\beta_2 < 0$, (see below) and we know already that $\alpha_2 < 0$. We can determine that this bifurcation occurs at

$$B_3^-: \quad (I_2)_{B_3^-} = \frac{\beta_1(\lambda\Lambda_1 - \sigma_4)}{4(\alpha_3\beta_1 - 2\alpha_2\beta_2)}.$$

In order for I_2 to be positive, we must have $\lambda < h\sigma_4/\Lambda_1$. Thus, B_3^- only exists for $\lambda < h\sigma_4/\Lambda_1$. By evaluating the eigenvalues of the system linearized about $PS2^-$ at point B_3^-, we can also determine that $PS2^-$ is stable before the bifurcation point (when it occurs), and unstable after the bifurcation point.

Here we make a brief diversion to prove that $\alpha_3\beta_1 - 2\alpha_2\beta_2 < 0$. For the pipe, if we write this combination of coefficients in terms of the physical parameters M_r, T, and κ, we obtain

$$\begin{aligned}\alpha_3\beta_1 - 2\alpha_2\beta_2 = &-\frac{81\kappa\pi^8\sqrt{\pi^2+\bar{T}}}{36M_r\Lambda_1^8} \times \{6561\pi^{10} + 917504M_r^6(\pi^2+\bar{T})^2 \\ &+ 7776M_r^2\pi^6(13\pi^2+\bar{T}) + 25344M_r^4(23\pi^6 + 22\pi^4\bar{T} - \pi^2\bar{T}^2)\}.\end{aligned}$$

We know that $\kappa > 0$, and we can show that if $-\pi^2 < \bar{T} < 23\pi^2$, then all of the summands in the numerator are positive. In this case, the whole coefficient $\alpha_3\beta_1 - 2\alpha_2\beta_2 < 0$. Of course, we remember that we defined our critical velocities by $u_0^2 = \pi^2 + \bar{T}$. Thus, if $\bar{T} < -\pi^2$, then our critical velocity is imaginary, i.e., there is no critical velocity. Thus, for the double zero eigenvalue case that we are considering, we must have $\bar{T} < -\pi^2$, and hence $\alpha_3\beta_1 - 2\alpha_2\beta_2 < 0$ for the pipe.

Table 1
Order of bifurcations of trivial solution as the parameter δ is increased

Parameter region	$(\beta_2 > 0)$	$(\beta_2 < 0)$
$\lambda < -\frac{\sigma_4}{\Lambda_1}$	$\{PS2^-, PS2^+, PS1\}$	$\{PS1, PS2^+, PS2^-\}$
$-\frac{\sigma_4}{\Lambda_1} < \lambda < \frac{\sigma_4}{\Lambda_1}$	$\{PS2^-, PS1, PS2^+\}$	$\{PS2^+, PS1, PS2^-\}$
$\lambda > \frac{\sigma_4}{\Lambda_1}$	$\{PS1, PS2^-, PS2^+\}$	$\{PS2^+, PS2^-, PS1\}$

Similarly, we can find the bifurcation point for $PS2^+$ to occur at

$$B_3^+: \quad \delta_{B_3^+} = \frac{-2\alpha_2(\lambda\Lambda_1 + \sigma_4)}{\alpha_3\beta_1 - 2\alpha_2\beta_2}$$

or

$$B_3^+: \quad (I_2)_{B_3^+} = \frac{\beta_1(\lambda\Lambda_1 + \sigma_4)}{4(\alpha_3\beta_1 - 2\alpha_2\beta_2)}.$$

Thus, B_3^+ only occurs for $\lambda < -\sigma_4/\Lambda_1$. Also, we can determine that solution $PS2^+$ is never stable.

Hence, we again have three cases for the second-mode solutions. In each case, $PS2^-$ occurs before $PS2^+$ for the pipe.

(i) First, if $\lambda < -\sigma_4/\Lambda_1$, then both $PS2^{\mp}$ bifurcate before $PS1$. Solution $PS2^-$ has a bifurcation point at B_3^-, and is stable before that bifurcation, and unstable afterwards. Solution $PS2^+$ has a bifurcation point at B_3^+, and is always unstable.

(ii) Second, if $-\sigma_4/\Lambda_1 < \lambda < \sigma_4/\Lambda_1$, then $PS2^-$ bifurcates before $PS1$, and $PS2^+$ bifurcates after $PS1$. Solution $PS2^-$ has a bifurcation at B_3^-, and is stable before that bifurcation, and unstable afterwards. Solution $PS2^+$ has no bifurcations, and is always unstable.

(iii) Finally, if $\lambda > \sigma_4/\Lambda_1$, then solutions $PS2^{\pm}$ both bifurcate after $PS1$. Neither of $PS2^{\pm}$ has bifurcations, and both solutions are always unstable.

These scenarios are shown schematically in Fig. 8.

5.2.3. Multi-mode solutions

Finally, we can determine the multi-mode solutions for this case, i.e., solutions of (16) for which the amplitude of both modes are nonzero. Due to the length of these expressions, we just write them in simpler action-angle coordinates, as

$$MM1: \quad I_1 = \frac{\delta(\alpha_3\beta_1 - 2\alpha_2\beta_2) + 2\alpha_2(\lambda\Lambda_1 - \sigma_4)}{16(\alpha_2^2 - 4\alpha_1\alpha_3)}, \quad \tan\theta_1 = 0,$$
$$I_2 = \frac{-\delta(\alpha_2\beta_1 - 8\alpha_1\beta_2) - 8\alpha_1(\lambda\Lambda_1 - \sigma_4)}{8(\alpha_2^2 - 4\alpha_1\alpha_3)}, \quad \tan\theta_2 = \frac{\sigma_4^i - \sigma_4}{\sigma_4^r};$$

$$MM2: \quad I_1 = \frac{\delta(\alpha_3\beta_1 - 2\alpha_2\beta_2) + 2\alpha_2(\lambda\Lambda_1 + \sigma_4)}{16(\alpha_2^2 - 4\alpha_1\alpha_3)}, \quad \tan\theta_1 = 0,$$
$$I_2 = \frac{-\delta(\alpha_2\beta_1 - 8\alpha_1\beta_2) - 8\alpha_1(\lambda\Lambda_1 + \sigma_4)}{8(\alpha_2^2 - 4\alpha_1\alpha_3)}, \quad \tan\theta_2 = \frac{\sigma_4^i + \sigma_4}{\sigma_4^r}.$$

We note that the phase coordinates do not change on the multi-mode solutions. We can also determine that solution $MM1$ connects B_2, the second bifurcation point of $PS1$ to B_3^-, the bifurcation point of $PS2^-$, and $MM2$ connects B_1, the first bifurcation point of $PS1$ to B_3^+, the bifurcation point of $PS2^+$. The existence of each multi-mode solution has the same criteria as the corresponding existence criteria of the bifurcation points that are its end points. Namely, for $\lambda > \sigma_4/\Lambda_1$, no multi-mode solutions exist, for $-\sigma_4/\Lambda_1 < \lambda < \sigma_4/\Lambda_1$, only $MM1$ exists, and for $\lambda < -\sigma_4/\Lambda_1$, both $MM1$ and $MM2$ exist. The multi-mode solutions are shown in Fig. 8.

The stability of these multi-mode solutions is very difficult to determine analytically, but we can determine it easily numerically for specific cases. We will postpone this determination of the stability until we study the damped system. We also note that the multi-modal solutions provide a mechanism for energy to be transferred from the high-frequency second mode to the low-frequency first mode. For values of δ at which $MM1$ exists, the second-mode solution $PS2^-$ is unstable. Thus, for initial conditions near $PS2^-$ the trajectories go towards the multi-modal solution $MM1$. This fact shows an energy transfer between the modes.

5.3. Forced system with linear damping

Next, we look at the system with only linear damping and forcing. The equations of motion in rectangular coordinates are

$$\dot{x}_1 = \beta_1\delta y_1 + 32\alpha_1 y_1^3 + 4\alpha_2 y_1(x_2^2 + y_2^2) + \zeta\delta_1 x_1,$$
$$\dot{y}_1 = x_1 + \zeta\delta_1 y_1,$$

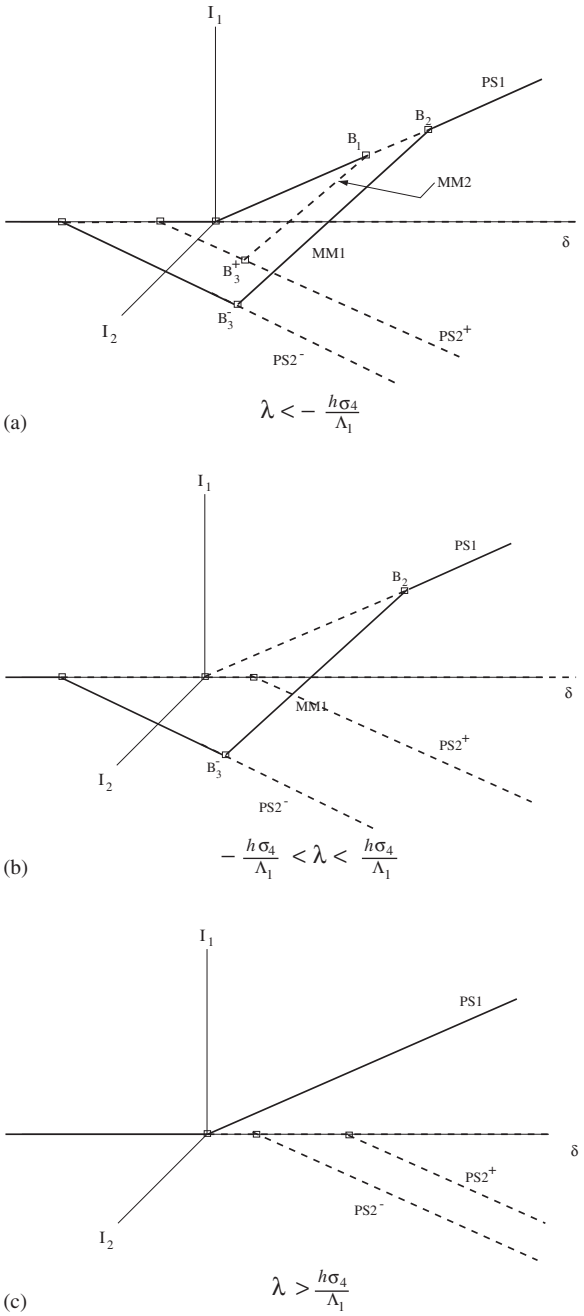

Fig. 8. Bifurcation scenarios for the pipe.

$$\dot{x}_2 = (\beta_2\delta - \lambda\Lambda_1)y_2 + 4\alpha_2 y_1^2 y_2 + 2\alpha_3 y_2(x_2^2 + y_2^2) + \zeta\delta_2 x_2 - \sigma_4^r x_2 + \sigma_4^i y_2,$$
$$\dot{y}_2 = -(\beta_2\delta - \lambda\Lambda_1)x_2 - 4\alpha_2 y_1^2 x_2 - 2\alpha_3 x_2(x_2^2 + y_2^2) + \zeta\delta_2 y_2 + \sigma_4^r y_2 + \sigma_4^i x_2. \tag{17}$$

First, we examine the stability of the trivial solution. By examining the characteristic equations of the Jacobian at $(x_1, y_1, x_2, y_2) = (0, 0, 0, 0)$, we can determine that the system undergoes a simple bifurcation into the

I_1 plane at

$$PS1: \quad \delta = \frac{\zeta^2\delta_1^2}{\beta_1}.$$

The system also undergoes simple bifurcations into the I_2 plane at

$$PS2^-: \quad \delta = \frac{\lambda\Lambda_1 - \sqrt{\sigma_4^2 - \zeta^2\delta_2^2}}{\beta_2} \quad \text{and} \quad PS2^+: \quad \delta = \frac{\lambda\Lambda_1 + \sqrt{\sigma_4^2 - \zeta^2\delta_2^2}}{\beta_2}.$$

These bifurcation points differ only slightly from the corresponding bifurcation points for the undamped system, assuming $\zeta \ll 1$. Thus for the trivial solution, we obtain stability diagrams in the $\delta - \lambda$ plane very similar to Fig. 7.

As for the undamped case, we can determine which bifurcation happens first—the bifurcation to the first mode or one of the bifurcations to the second mode. The bifurcation to the first mode always occurs for $\delta > 0$, while the bifurcations to the second mode may occur for $\delta < 0$ or $\delta > 0$. There are three possibilities, as for the undamped case, if we ignore degenerate cases at which two of these bifurcation points coalesce. These cases are summarized in Table 2, where the second and third columns give the order of the bifurcations as the parameter δ is increased. It may also happen that two of these bifurcation points occur simultaneously, i.e. $\{PS1, PS2^-\}$ or $\{PS1, PS2^+\}$ bifurcate from the trivial solution at the same value of δ. Although we do not study such degenerate points here, we note that this behavior will occur at

$$\lambda = \frac{\dfrac{\beta_2\zeta^2\delta_1^2}{\beta_1} \mp \sqrt{\sigma_4^2 - \zeta^2\delta_2^2}}{\Lambda_1}.$$

5.3.1. First-mode solutions

Next, we look for solutions with $x_2 = y_2 = 0$. In this case, the solutions are nearly the same as the first-mode solutions for the unforced case, namely

$$PS1: \quad (x_1, y_1) = \left(\mp\zeta\delta_1 \sqrt{\frac{\zeta^2\delta_1^2 - \beta_1\delta}{32\alpha_1}}, \pm\sqrt{\frac{\zeta^2\delta_1^2 - \beta_1\delta}{32\alpha_1}} \right) = (\mp\zeta\delta_1 y_{10}, \pm y_{10}).$$

The solutions only exist for

$$PS1 \text{ exists if:} \quad \delta > \frac{\zeta^2\delta_1^2}{\beta_1},$$

and thus the branches are supercritical. To determine the stability of the first-mode solution $PS1$, we use the equations of motion in coordinates (x_1, y_1, x_2, y_2), and determine the Jacobian evaluated on $PS1$. Using the Routh Hurwitz criterion, we can show that this branch does not become unstable with respect to the I_1 plane, but does become unstable with respect to the I_2 plane, with simple bifurcation points B_1 and B_2 at

$$B_1: \quad \delta = \frac{\alpha_2\zeta^2\delta_1^2 + 8\alpha_1\left(-\lambda\Lambda_1 - \sqrt{\sigma_4^2 - \zeta^2\delta_2^2}\right)}{(\alpha_2\beta_1 - 8\alpha_1\beta_2)},$$

Table 2
Order of bifurcations of trivial solution for forced system with linear damping

Parameter region	$(\beta_2 > 0)$	$(\beta_2 < 0)$
$\lambda < \dfrac{\frac{\beta_2\zeta^2\delta_1^2}{\beta_1} - \sqrt{\sigma_4^2 - \zeta^2\delta_2^2}}{\Lambda_1}$	$\{PS2^-, PS2^+, PS1\}$	$\{PS1, PS2^+, PS2^-\}$
$\dfrac{\frac{\beta_2\zeta^2\delta_1^2}{\beta_1} - \sqrt{\sigma_4^2 - \zeta^2\delta_2^2}}{\Lambda_1} < \lambda < \dfrac{\frac{\beta_2\zeta^2\delta_1^2}{\beta_1} + \sqrt{\sigma_4^2 - \zeta^2\delta_2^2}}{\Lambda_1}$	$\{PS2^-, PS1, PS2^+\}$	$\{PS2^+, PS1, PS2^-\}$
$\lambda > \dfrac{\frac{\beta_2\zeta^2\delta_1^2}{\beta_1} + \sqrt{\sigma_4^2 - \zeta^2\delta_2^2}}{\Lambda_1}$	$\{PS1, PS2^-, PS2^+\}$	$\{PS2^+, PS2^-, PS1\}$

$$B_2: \quad \delta = \frac{\alpha_2\zeta^2\delta_1^2 + 8\alpha_1\left(-\lambda\Lambda_1 + \sqrt{\sigma_4^2 - \zeta^2\delta_2^2}\right)}{(\alpha_2\beta_1 - 8\alpha_1\beta_2)}.$$

We can show that for the pipe the combination of coefficients $\alpha_2\beta_1 - 8\alpha_1\beta_2$ is given by

$$\alpha_2\beta_1 - 8\alpha_1\beta_2 = -\frac{9\pi^{12}\kappa\omega_1(32M_r^2\Lambda_1^2 + 9\pi^2\omega_1^2)}{2M_r^2\Lambda_1^7} < 0.$$

The bifurcation point B_1 occurs at a lower value of δ than B_2, so we say that B_1 occurs first.

Next, we can give the values of the action I_1 at which these two bifurcation points occur. We calculate

$$I_1^{B_1} = \frac{(\zeta^2\delta_1^2 + 1)\left(-\beta_2\zeta^2\delta_1^2 + \beta_1\left(\lambda\Lambda_1 + \sqrt{\sigma_4^2 - \zeta^2\delta_2^2}\right)\right)}{8(\alpha_2\beta_1 - 8\alpha_1\beta_2)}$$

and

$$I_1^{B_2} = \frac{(\zeta^2\delta_1^2 + 1)\left(-\beta_2\zeta^2\delta_1^2 + \beta_1\left(\lambda\Lambda_1 - \sqrt{\sigma_4^2 - \zeta^2\delta_2^2}\right)\right)}{8(\alpha_2\beta_1 - 8\alpha_1\beta_2)}.$$

Again, due to the fact that $\alpha_2\beta_1 - 8\alpha_1\beta_2 < 0$, we can see that B_1 occurs for the lower value of I_1.

Of course, we need to ensure that these bifurcation points occur for $I_1 > 0$, since branch $PS1$ does not exist elsewhere. Thus, the bifurcations will occur only if

$$B_1 \text{ exists:} \quad \lambda < \frac{\dfrac{\beta_2\zeta^2\delta_1^2}{\beta_1} - \sqrt{\sigma_4^2 - \zeta^2\delta_2^2}}{\Lambda_1},$$

$$B_2 \text{ exists:} \quad \lambda < \frac{\dfrac{\beta_2\zeta^2\delta_1^2}{\beta_1} + \sqrt{\sigma_4^2 - \zeta^2\delta_2^2}}{\Lambda_1}.$$

Finally, we can determine the stability of branch $PS1$. We know that a branch can only change stability at one of its bifurcation points. To determine stability, we use the Routh–Hurwitz method. Since the characteristic equation can be decomposed into two quadratic equations, the Routh–Hurwitz criterion reduces to the requirement that all the coefficients of these two characteristic equations have the same sign. Thus, we hav the two characteristic equations

$$s^2 + b_1 s + c_1 = 0 \quad \text{and} \quad s^2 + b_2 s + c_2 = 0,$$

where the first equation corresponds to the first mode, and the second equation corresponds to the second mode. The coefficients are

$$b_1 = -2\zeta\delta_1, \quad c_1 = 2(-\zeta^2\delta_1^2 + \beta_1\delta) \quad \text{and} \quad b_2 = -2\zeta\delta_2, \quad c_2 = C_1\delta^2 + C_2\delta + C_3.$$

The two coefficients b_1 and b_2 are always positive, since $\delta_1 < 0$ and $\delta_2 < 0$, so there are no Hopf bifurcations. The coefficient $c_1 > 0$ for $\delta > \zeta^2\delta_1^2/\beta_1$, which is where $PS1$ exists, so c_1 is always positive on $PS1$. For the coefficient c_2, we note that $c_2 = 0$ at the two bifurcation points B_1 and B_2. Furthermore, the curve $c_2 = c_2(\delta)$ is a quadratic function of δ with

$$C_1 = \frac{(\alpha_2\beta_1 - 8\alpha_1\beta_2)^2}{64\alpha_1^2} > 0.$$

Thus, the curve $c_2 = c_2(\delta)$ is concave upwards. This means that c_2 is only less than zero between the two bifurcation points, and greater than zero otherwise. Thus, when B_1 and B_2 both exist, $PS1$ is initially stable, becomes unstable at B_1, and restabilizes at B_2. When only B_2 exists, $PS1$ is initially unstable, and stabilizes at B_2. In this case, we consider B_1 to occur for $I_1 < 0$. If neither B_1 nor B_2 exists, then $PS1$ is always stable. In this case, we consider B_1 and B_2 to both occur for $I_1 < 0$.

5.3.2. Second-mode solutions

Next, we look for solutions with $x_1 = y_1 = 0$ and $I_2 \neq 0$. For convenience, we transform (17) to coordinates $(x_1, y_1, I_2, \theta_2)$:

$$\begin{aligned}
\dot{x}_1 &= \beta_1\delta y_1 + 32\alpha_1 y_1^3 + 8\alpha_2 y_1 I_2 + \zeta\delta_1 x_1,\\
\dot{y}_1 &= x_1 + \zeta\delta_1 y_1,\\
\dot{I}_2 &= 2\zeta\delta_2 I_2 + 2I_2(\sigma_4^r \cos 2\theta_2 + \sigma_4^i \sin 2\theta_2),\\
\dot{\theta}_2 &= \beta_2\delta - \lambda\Lambda_1 + 4\alpha_3 I_2 + (\sigma_4^i \cos 2\theta_2 - \sigma_4^r \sin 2\theta_2).
\end{aligned} \tag{18}$$

Solving for fixed points of these equations with $x_1 = y_1 = 0$, we obtain two branches, denoted $PS2^-$ and $PS2^+$:

$$PS2^-: \quad I_2 = \frac{(\lambda\Lambda_1 - \beta_2\delta) - \sqrt{\sigma_4^2 - \zeta^2\delta_2^2}}{4\alpha_3},$$

$$PS2^+: \quad I_2 = \frac{(\lambda\Lambda_1 - \beta_2\delta) + \sqrt{\sigma_4^2 - \zeta^2\delta_2^2}}{4\alpha_3}.$$

Since we must have $I_2 > 0$ for a solution to exist, we obtain the following conditions for these solutions to exist:

$$PS2^-: \quad \delta > \frac{\lambda\Lambda_1 - \sqrt{\sigma_4^2 - \zeta^2\delta_2^2}}{\beta_2} \quad \text{and} \quad PS2^+: \quad \delta > \frac{\lambda\Lambda_1 + \sqrt{\sigma_4^2 - \zeta^2\delta_2^2}}{\beta_2}.$$

For the pipe, $PS2^-$ and $PS2^+$ correspond to two parallel lines in the $I_2 - \delta$ plane, each with positive slope (since $\alpha_3 < 0$, $\beta_2 > 0$). Thus, the branches are supercritical. We also note that, for a given value of δ, $I_2^{PS2^+} < I_2^{PS2^-}$, since $\alpha_3 < 0$ when both exist. The existence of these solutions is of course contingent upon the condition $\zeta^2\delta_2^2 < \sigma_4^2$. As for the undamped case, the branch $PS2^-$ occurs first for the pipe, while $PS2^+$.

Next, we can examine the stability of the solutions $PS2^\pm$. Using the Routh–Hurwitz methods described earlier, we determine that solution $PS2^-$ may undergo a simple bifurcation into the plane of the first mode at

$$B_3^-: \quad \delta = \frac{\alpha_3\delta_1^2 + 2\alpha_2\left(-\lambda\Lambda_1 + \sqrt{\sigma_4^2 - \zeta^2\delta_2^2}\right)}{(\alpha_3\beta_1 - 2\alpha_2\beta_2)}$$

and solution $PS2^+$ may undergo a simple bifurcation into the plane of the first-mode solution at

$$B_3^+: \quad \delta = \frac{\alpha_3\delta_1^2 + 2\alpha_2\left(-\lambda\Lambda_1 - \sqrt{\sigma_4^2 - \zeta^2\delta_2^2}\right)}{(\alpha_3\beta_1 - 2\alpha_2\beta_2)}.$$

We showed earlier that $\alpha_3\beta_1 - 2\alpha_2\beta_2 < 0$ for both the pipe and shaft. Thus B_3^+ occurs for a lower value of δ than B_3^- (when both exist). We next determine what values of I_2 the bifurcations from each of the branches occurs at. First, for branch $PS2^-$, the bifurcation B_3^- occurs at

$$B_3^-: \quad I_2 = \frac{-\beta_2\zeta^2\delta_1^2 + \beta_1\left(\lambda\Lambda_1 - \sqrt{\sigma_4^2 - \zeta^2\delta_2^2}\right)}{4(\alpha_3\beta_1 - 2\alpha_2\beta_2)}.$$

For branch $PS2^+$, the bifurcation B_3^+ occurs at

$$B_3^+: \quad I_2 = \frac{-\beta_2\zeta^2\delta_1^2 + \beta_1\left(\lambda\Lambda_1 + \sqrt{\sigma_4^2 - \zeta^2\delta_2^2}\right)}{4(\alpha_3\beta_1 - 2\alpha_2\beta_2)}.$$

Thus, B_3^+ will occur at a lesser value of I_2 than B_3^-.

Using the fact that $I_2 > 0$, we determine the following existence criteria for the bifurcation points B_3^- and B_3^+:

$$B_3^- \text{ exists:} \quad \lambda < \frac{\dfrac{\beta_2\zeta^2\delta_1^2}{\beta_1} + \sqrt{\sigma_4^2 - \zeta^2\delta_2^2}}{\Lambda_1};$$

$$B_3^+ \text{ exists:} \quad \lambda < \frac{\dfrac{\beta_2\zeta^2\delta_1^2}{\beta_1} - \sqrt{\sigma_4^2 - \zeta^2\delta_2^2}}{\Lambda_1}.$$

Next, we discuss the stability of these branches. For $PS2^-$, the important quantity in the Routh–Hurwitz table is

$$c_1 = \frac{\alpha_3(\delta_1^2 - \beta_1\delta) + 2\alpha_2\left(\beta_2\delta - \lambda\Lambda_1 + \sqrt{\sigma_4^2 - \zeta^2\delta_2^2}\right)}{\alpha_3}.$$

If $c_1 > 0$, then $PS2^-$ is stable, while if $c_1 < 0$, $PS2^+$ is unstable. We calculate that $c_1 = 0$ at $\delta = B_3^-$, which is the bifurcation point at which $PS2^-$ changes stability. In addition

$$\frac{\mathrm{d}c_1}{\mathrm{d}\delta} = -\frac{(\alpha_3\beta_1 - 2\alpha_2\beta_2)}{\alpha_3} < 0,$$

so c_1 decreases monotonically. Therefore, we have that $c_1 > 0$ (stable) for $\delta < \delta_{B_3^-}$ and $c_1 < 0$ (unstable) for $\delta > \delta_{B_3^-}$. Thus, for both the pipe and shaft, $PS2^-$ is stable for $\delta < \delta_{B_3^-}$. Using a similar argument, we can show that the solution $PS2^+$ will always be unstable, for both the pipe and the shaft.

5.3.3. Multi-mode solutions

Since there are no multi-mode solutions present in the unforced case, it is clear that any multi-mode solutions will be due to the forcing. Since the first-mode solutions may have simple bifurcations into the I_2 plane, and the second-mode solutions may each have a simple bifurcation into the I_1 plane, we expect that multi-mode solutions would originate from those bifurcation points, if they exist. In this case, the equations to be solved are (18). To solve these equations, we first solve the $\dot{y}_1$ equation for x_1 as $x_1 = -\zeta\delta_1 y_1$. We then substitute this into the equation $\dot{x}_1 = 0$ and solve for y_1 to obtain

$$y_1 \stackrel{\text{def}}{=} \pm y_{10} = \pm\sqrt{\frac{\zeta^2\delta_1^2 - 8\alpha_2 I_2 - \beta_1\delta}{32\alpha_1}}$$

and consequently

$$x_1 = \mp\zeta\delta_1\sqrt{\frac{\zeta^2\delta_1^2 - 8\alpha_2 I_2 - \beta_1\delta}{32\alpha_1}} = \mp\zeta\delta_1 y_{10}.$$

Thus, we have the two solutions $(x_1, y_1) = (-\zeta\delta_1 y_{10}, y_{10})$ and $(x_1, y_1) = (\zeta\delta_1 y_{10}, -y_{10})$. More conveniently, we obtain

$$y_{10}^2 = \frac{\zeta^2\delta_1^2 - 8\alpha_2 I_2 - \beta_1\delta}{32\alpha_1}.$$

We next substitute this expression for y_0^2 into the equations for the second mode, to obtain expressions for I_2 as

$$MM1: \quad I_2 = \frac{\alpha_2(\zeta^2\delta_1^2 - \beta_1\delta) - 8\alpha_1\left(\lambda\Lambda_1 - \beta_2\delta - \sqrt{\sigma_4^2 - \zeta^2\delta_2^2}\right)}{8(\alpha_2^2 - 4\alpha_1\alpha_3)}$$

and

$$MM2: \quad I_2 = \frac{\alpha_2(\zeta^2\delta_1^2 - \beta_1\delta) - 8\alpha_1\left(\lambda\Lambda_1 - \beta_2\delta + \sqrt{\sigma_4^2 - \zeta^2\delta_2^2}\right)}{8(\alpha_2^2 - 4\alpha_1\alpha_3)}.$$

So we have two solutions, where we have assumed that $\alpha_2^2 - 4\alpha_1\alpha_3 > 0$. Finally, we can substitute this expression for I_2 back into the expressions for x_1 and y_1, and use $I_1 = (x_1^2 + y_1^2)/2$ to obtain the two corresponding expressions for I_1 as

$$MM1: \quad I_1 = \frac{(\zeta^2\delta_1^2 + 1)\left(\alpha_3(\beta_1\delta - \zeta^2\delta_1^2) + 2\alpha_2\left(\lambda\Lambda_1 - \beta_2\delta - \sqrt{\sigma_4^2 - \zeta^2\delta_2^2}\right)\right)}{16(\alpha_2^2 - 4\alpha_1\alpha_3)},$$

$$MM2: \quad I_1 = \frac{(\zeta^2\delta_1^2 + 1)\left(\alpha_3(\beta_1\delta - \zeta^2\delta_1^2) + 2\alpha_2\left(\lambda\Lambda_1 - \beta_2\delta + \sqrt{\sigma_4^2 - \zeta^2\delta_2^2}\right)\right)}{16(\alpha_2^2 - 4\alpha_1\alpha_3)}.$$

Next, we can verify that these solutions do connect the single-mode solutions to each other. As for the undamped case, $MM1$ connects B_3^- on $PS2^-$ to B_2, the second bifurcation point on $PS1$, and $MM2$ connects B_3^+ on $PS2^+$ to B_1, the first bifurcation point on $PS1$.

Finally, we can determine the stability of the two multi-mode solutions. The Routh–Hurwitz criteria for the multi-mode solutions is too complicated to be determined analytically, but we will be able to see the stability of these solutions numerically. From our observations, we can say that the solution $MM1$ seems to be stable, while $MM2$ is unstable (when each of these exists). Also, $MM2$ may have a pair of imaginary eigenvalues crossing into the right half plane, but since this solution is already unstable, this is not a Hopf bifurcation.

Next, we show some example plots for the pipe, generated using the numerical bifurcation package AUTO97 (Doedel et al., 1997). Plots for the case $M_r = 0.7$, $\bar{T} = 0$, $\zeta = 0.01$, $\kappa = 2$, $h = 0.1$, and $\lambda = -0.1$ are given in Figs. 9 and 10. In all of these plots, stable solutions are shown with solid lines, unstable solutions with dotted lines. Plots for the case $M_r = 0.7$, $\bar{T} = 0$, $\zeta = 0.01$, $\kappa = 2$, $h = 0.1$, and $\lambda = 0.0$ are given in Figs. 11 and 12. Plots for the case $M_r = 0.7$, $\bar{T} = 0$, $\zeta = 0.01$, $\kappa = 2$, $h = 0.1$, and $\lambda = 0.0$ are given in Figs. 13 and 14.

In Figs. 9, 11 and 13, we plot the magnitude of the equilibrium solutions. The order of the bifurcations for the three cases are as shown in Table 2. In addition, all of the primary branches are supercritical, as expected. The two multi-mode solutions $MM1$ and $MM2$ are also shown, and connect the primary branches. From these diagrams, we see that (when they exist) $MM1$ is stable, while $MM2$ is unstable and has two points at which a pair of eigenvalues are crossing the imaginary axis (indicated by solid boxes). In Figs. 10, 12, and 14 we plot the coordinates of the equilibrium solutions versus δ. In each of these plots, the relevant single-mode solutions and the multi-mode solutions are shown and labelled. In the plots of x_2 and y_2, one of the second-mode solutions and one of the multi-mode solutions is difficult to see, since they are small compared to the corresponding other solution.

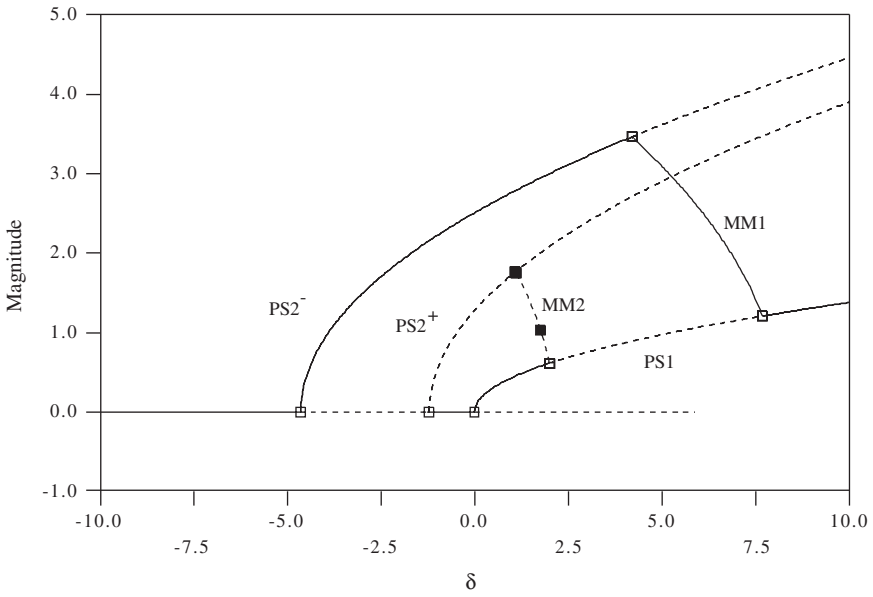

Fig. 9. Magnitude of response versus δ for $M_r = 0.7$, $\bar{T} = 0$, $\zeta = 0.01$, $\kappa = 2$, $h = 0.1$, and $\lambda = -0.1$.

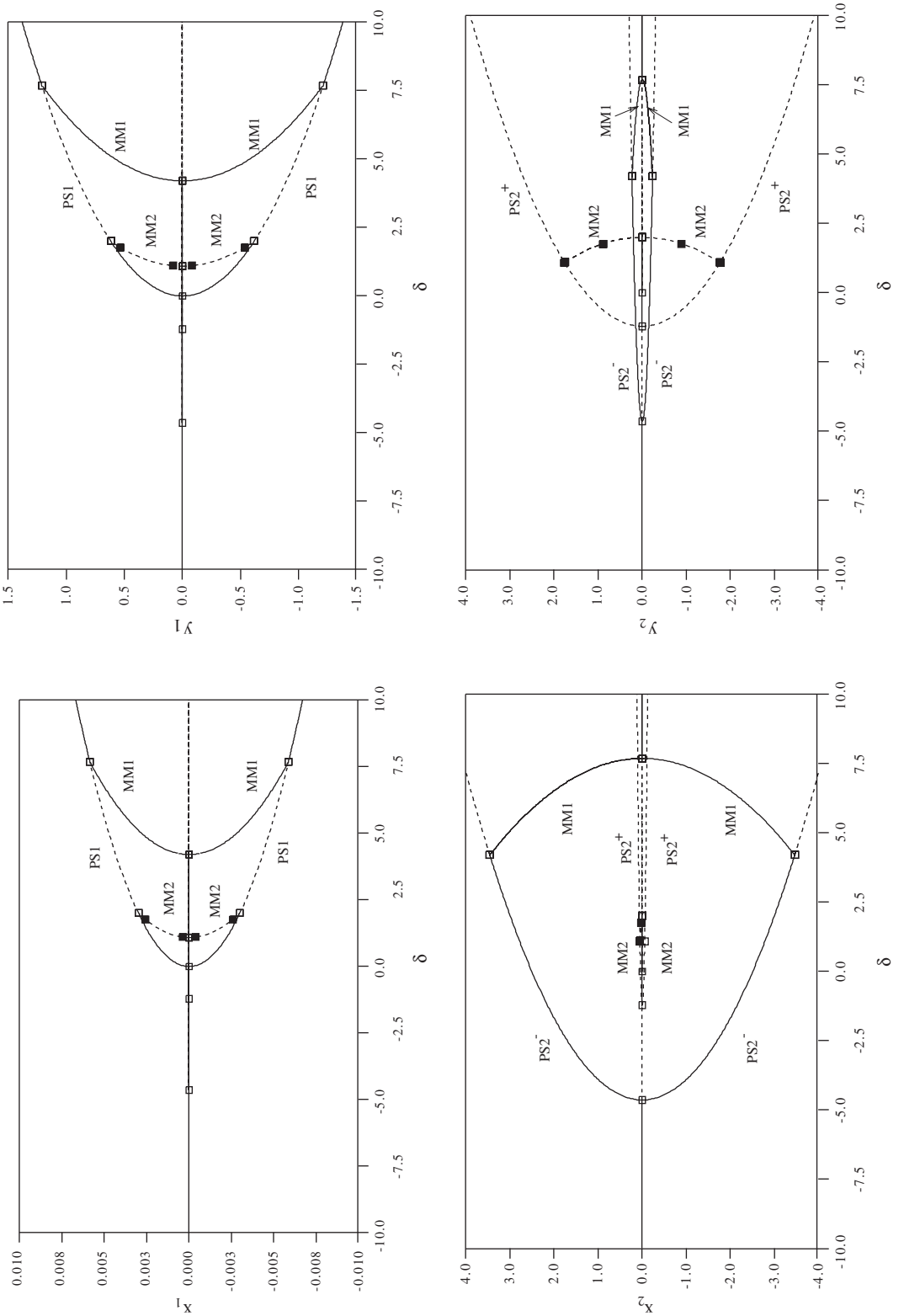

Fig. 10. Plots of coordinates versus δ for the same conditions as Fig. 9.

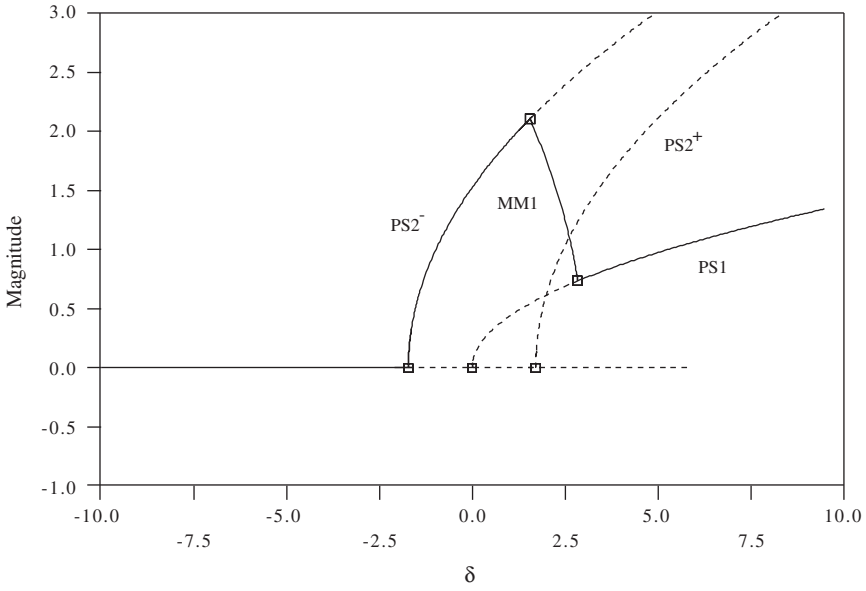

Fig. 11. Magnitude of response versus δ for $M_r = 0.7$, $\bar{T} = 0$, $\zeta = 0.01$, $\kappa = 2$, $h = 0.1$, and $\lambda = 0.0$.

Note that the behavior observed for the forced system with damping is qualitatively similar to the behavior shown in Fig. 8 for the forced pipe with no damping. This similarity was expected, since the linearly damped system had qualitatively the same features as the undamped system.

We can also see the phenomenon of energy transfer from the second mode to the first mode in these figures. The forcing excites the second mode and creates the second-mode solutions $PS2^-$ and $PS2^+$. Consider only the branch $PS2^-$. For $\delta < \delta_{B_3^-}$, the branch $PS2^-$ is stable, but for $\delta > \delta_{B_3^-}$, branch $PS2^-$ is unstable, and initial conditions near this unstable branch develop a component in the first mode as they move away from $PS2^-$. Thus, the forcing may cause an initial condition with $I_1 = 0$ to develop a component in the first mode, and hence we say that the energy input by the forcing is transferred from the second mode to the first mode. To understand the dynamics further, we will need to use the results of the global analysis in McDonald and Namachchivaya (2005).

5.4. Full equations of motion

Finally, we look at the most general form of the equations of motion. Thus, we consider the nonlinear system with forcing, and with both linear and nonlinear damping. These equations are the most difficult to analyze, so we will not be able to do much analytically. We will, however, show some numerical results for several cases. The stability results of the previous section, for the forced system with only linear damping, are still valid. The nonlinear damping only affects the primary bifurcation branches, their stability, and any multi-mode solutions.

Based on our previous results, we know the following.

(a) Second-mode solutions occur as a result of the subharmonic resonant forcing. Thus, we can expect second-mode solutions for the full equations of motion.
(b) The addition of nonlinear damping allowed the first-mode solution in the unforced case to undergo a Hopf bifurcation. Thus, the first-mode solution may have a Hopf bifurcation for the forced system.
(c) The addition of nonlinear damping will may connect the two second-mode branches at some higher value of δ. These branches were parallel when the system had only linear damping.

As mentioned, the linear stability results are the same as for the forced case with linear damping only. Thus, we have three bifurcation points of the trivial solution, leading to one first-mode solution and two second-mode solutions. The order of the bifurcations is as described in Table 2.

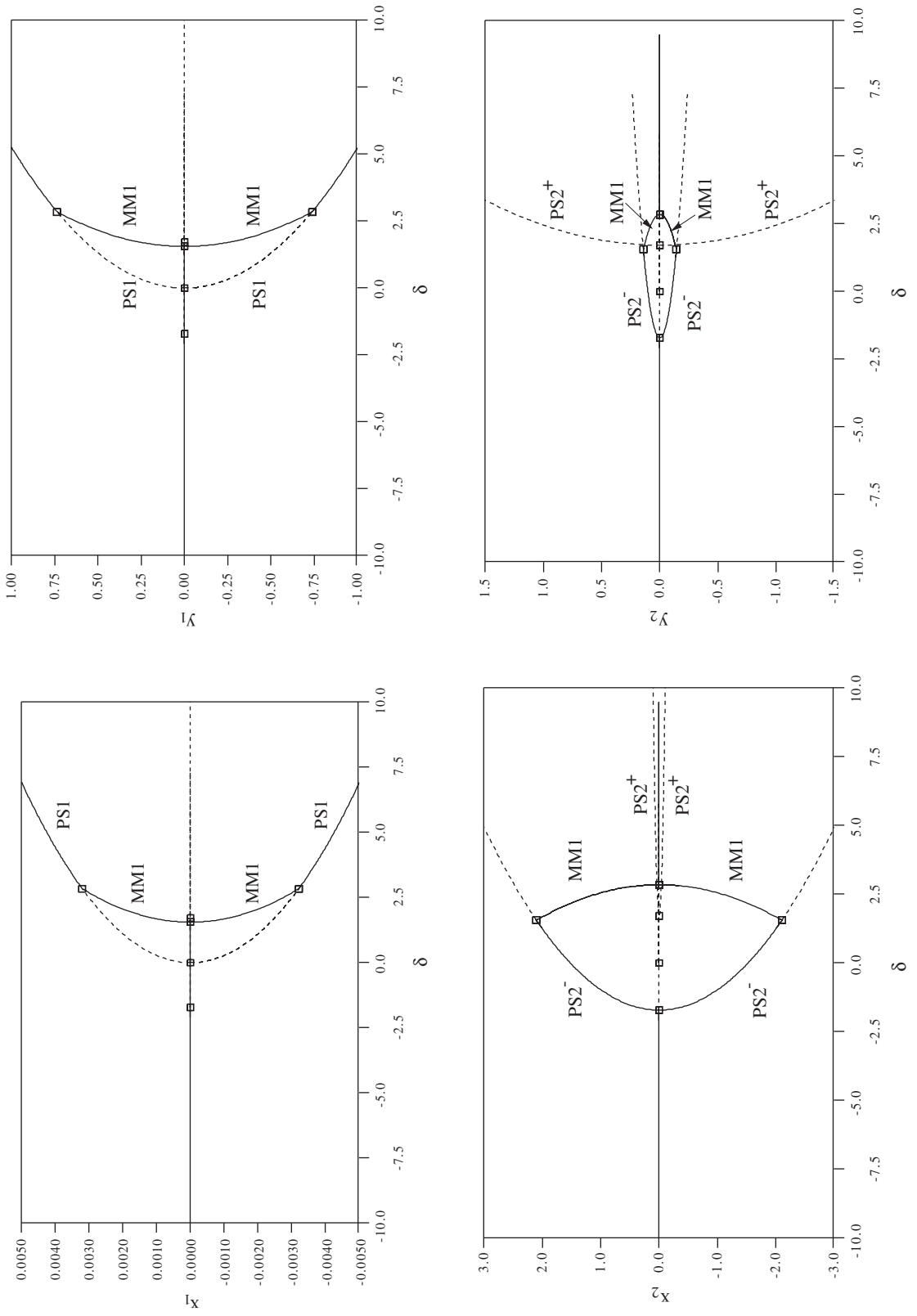

Fig. 12. Plots of coordinates versus δ for the same conditions as Fig. 11.

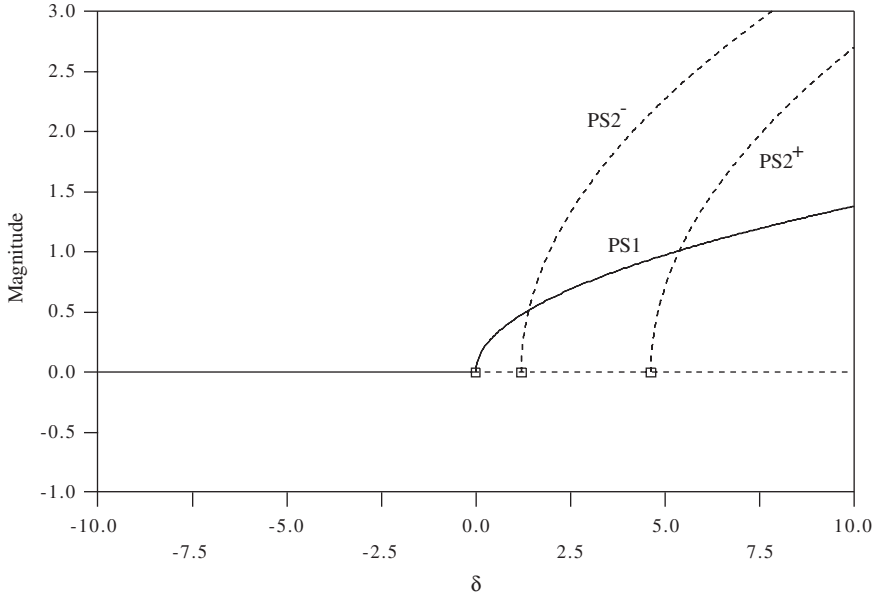

Fig. 13. Magnitude of response versus δ for $M_r = 0.7$, $\bar{T} = 0$, $\zeta = 0.01$, $\kappa = 2$, $h = 0.1$, and $\lambda = 0.0$.

5.4.1. First-mode solutions

Since the forcing is subharmonic, it only affects the second mode, and thus, the form of the first-mode branch is unchanged from the unforced case discussed in Section 5.1. As before, we can also show that branch $PS1$ does not have a simple bifurcation to the first mode for $\zeta \ll 1$, but may have a Hopf bifurcation to the first or second mode. The Hopf bifurcation to the first mode and second mode occur at the same points as those given in Section 5.1. Thus, the forcing does not affect the presence of a Hopf bifurcation. The condition for a simple bifurcation to the second mode to occur is much more complicated, and involves the forcing coefficient σ_4. We cannot solve this condition explicitly for δ, so we will not give this condition here. However, we may use AUTO97 (Doedel et al., 1997) to detect parameter values at which the first-mode solution undergoes a simple bifurcation into the plane of the second mode.

5.4.2. Second-mode solutions

Again, we can find expressions for the second-mode solutions. These expressions become rather unwieldy for the forced, nonlinearly damped problem, and it becomes rather difficult to answer stability questions for these branches. Thus, we will only be able to examine these solutions numerically. As for the system with linear damping only, we obtain two second-mode branches in the action-angle coordinates.

5.4.3. Multi-mode solutions

As for the second-mode solutions, any description of multi-mode solutions and their existence criteria will be extremely complicated and long. Thus, we will only be able to study these solutions numerically.

5.5. Numerical results

Since it is difficult to analytically determine stability, bifurcation points, etc. for the full system (13) with forcing and nonlinear damping, we rely on numerical tools, such as AUTO97 (Doedel et al., 1997). Although AUTO97 can only provide bifurcation diagrams for specific sets of parameters, it is helpful in determining what kind of behavior can be expected from the system. In these diagrams, stable solutions are shown with solid lines, unstable solutions with dotted lines. Simple bifurcations are indicated by empty boxes, Hopf bifurcations by solid boxes. Periodic solutions are indicated by circles, solid for stable solutions, and empty for unstable solutions.

Since we can only use AUTO97 to study the bifurcations for a specific set of parameters, it is difficult to understand the complete bifurcation picture of the system. However, we can see the types of bifurcations that occur for various parameter values. One example is given below.

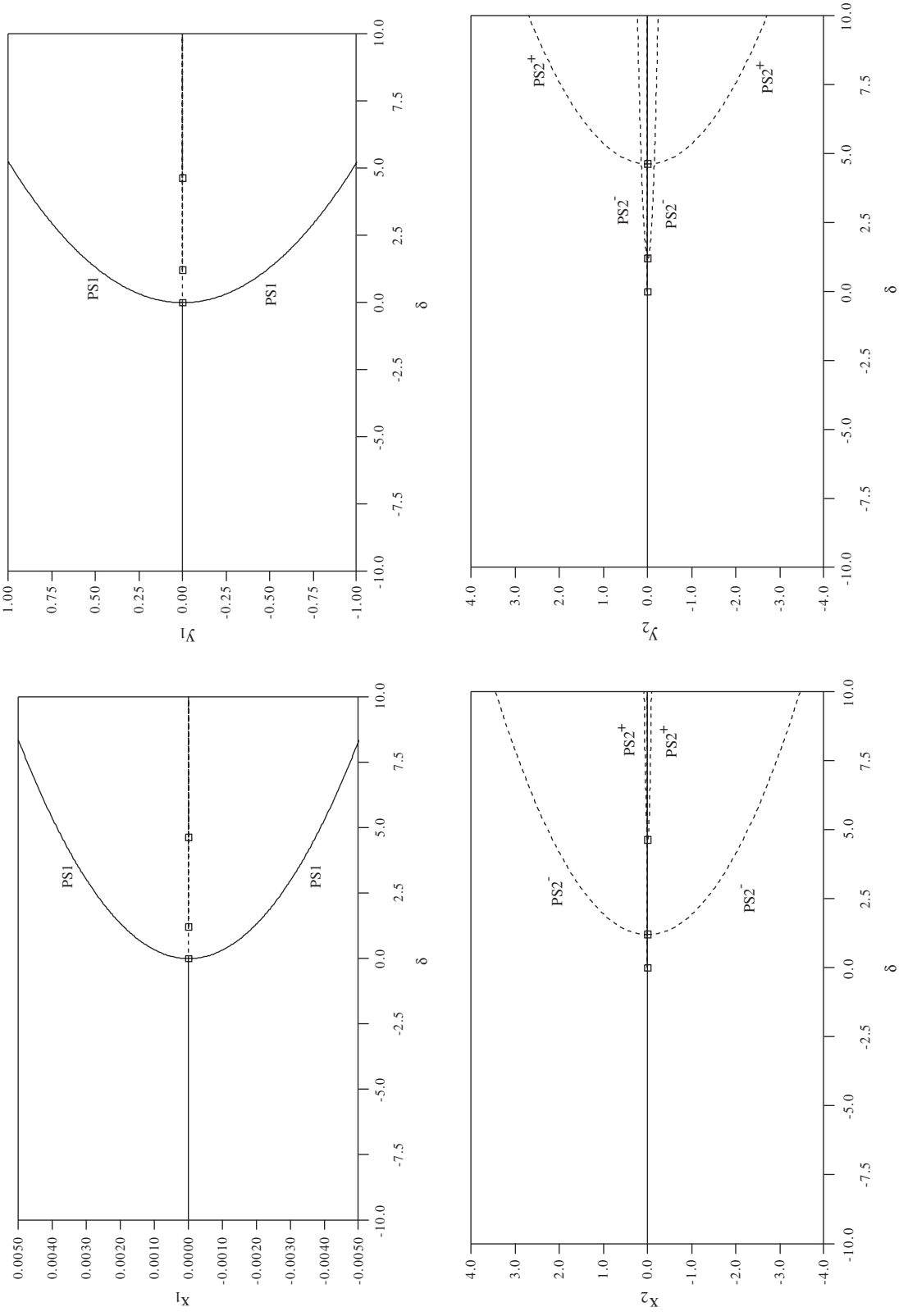

Fig. 14. Plots of coordinates versus δ for the same conditions as Fig. 13.

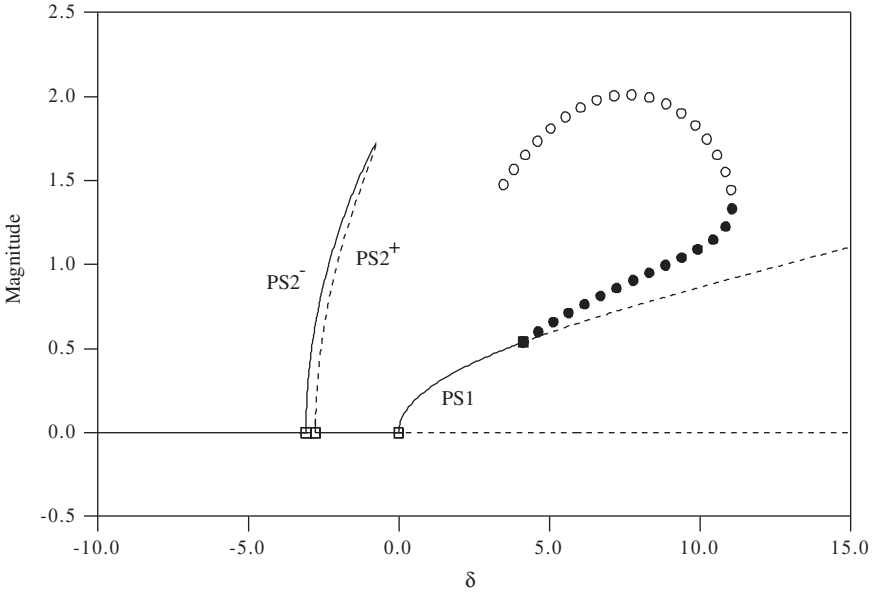

Fig. 15. Magnitude of response versus δ for $M_r = 0.7$, $\bar{T} = 0$, $\zeta^* = 0.01$, $\kappa = 2$, $\sigma = 0.01$, $h = 0.01$, and $\lambda = -0.1$.

Example for $M_r = 0.7$, $\bar{T} = 0$, $\zeta^* = 0.01$, $\kappa = 2$, $\sigma = 0.01$, $h = 0.01$, and $\lambda = -0.1$; see Figs. 15 and 16. In this case, the two second-mode solutions bifurcate first from the trivial solution, one stable, the other unstable. These two branches meet at a larger value of δ. One first-mode solution also bifurcates from the trivial solution, and undergoes a Hopf bifurcation. The periodic solution is initially stable, but has a limit point, at which the stability changes.

6. Conclusions

We can now summarize the results of the local bifurcation analysis. For the unforced case, there are no second-mode solutions, and the first-mode solution becomes unstable near $\delta = 0$. The first mode corresponds to the eigenvalues near zero in our original system, while the second mode corresponds to the eigenvalues that are far from zero on the imaginary axis.

When we add forcing at the subharmonic resonance frequency, we add *time-dependent* terms to the equations of motion. To study this system, we then made a time-dependent transformation that eliminates the explicit time dependence from the equations of motion. This transformation also moves the eigenvalue pair that was far from zero on the imaginary axis to the neighborhood of zero. If we had made this transformation for the unforced system, these eigenvalues would simply pass at zero as δ varied, due to the S^1-symmetry of the second mode. However, the addition of forcing breaks this symmetry, and hence the second mode can become unstable here. In fact, this behavior of the second mode is similar to the behavior of our gyroscopic system as a whole: symmetry-breaking causes an instability in the system, followed by a restabilization. Of course, the system cannot be restabilized if the first mode has already become unstable.

The behavior of the nontrivial solutions for the pipe, that is, each of the primary bifurcations is supercritical. For the system, there may be 0, 1, or 2 multi-mode solutions connecting the primary bifurcation branches, depending on the magnitude of the detuning parameter λ.

Our final results for the full system show the importance of higher order terms in determining the local bifurcation behavior. When we did not include nonlinear damping, the first-mode bifurcation branch only became unstable through a simple bifurcation, creating a multi-mode solution that connected to a primary second-mode bifurcation branch. When nonlinear damping terms were included, the first-mode branch became unstable through a Hopf bifurcation in the numerical example studied. However, the earlier results are not meaningless, for they provide a good approximation to the behavior for weakly damped systems. In addition, the presence of multi-mode solutions allows us to determine

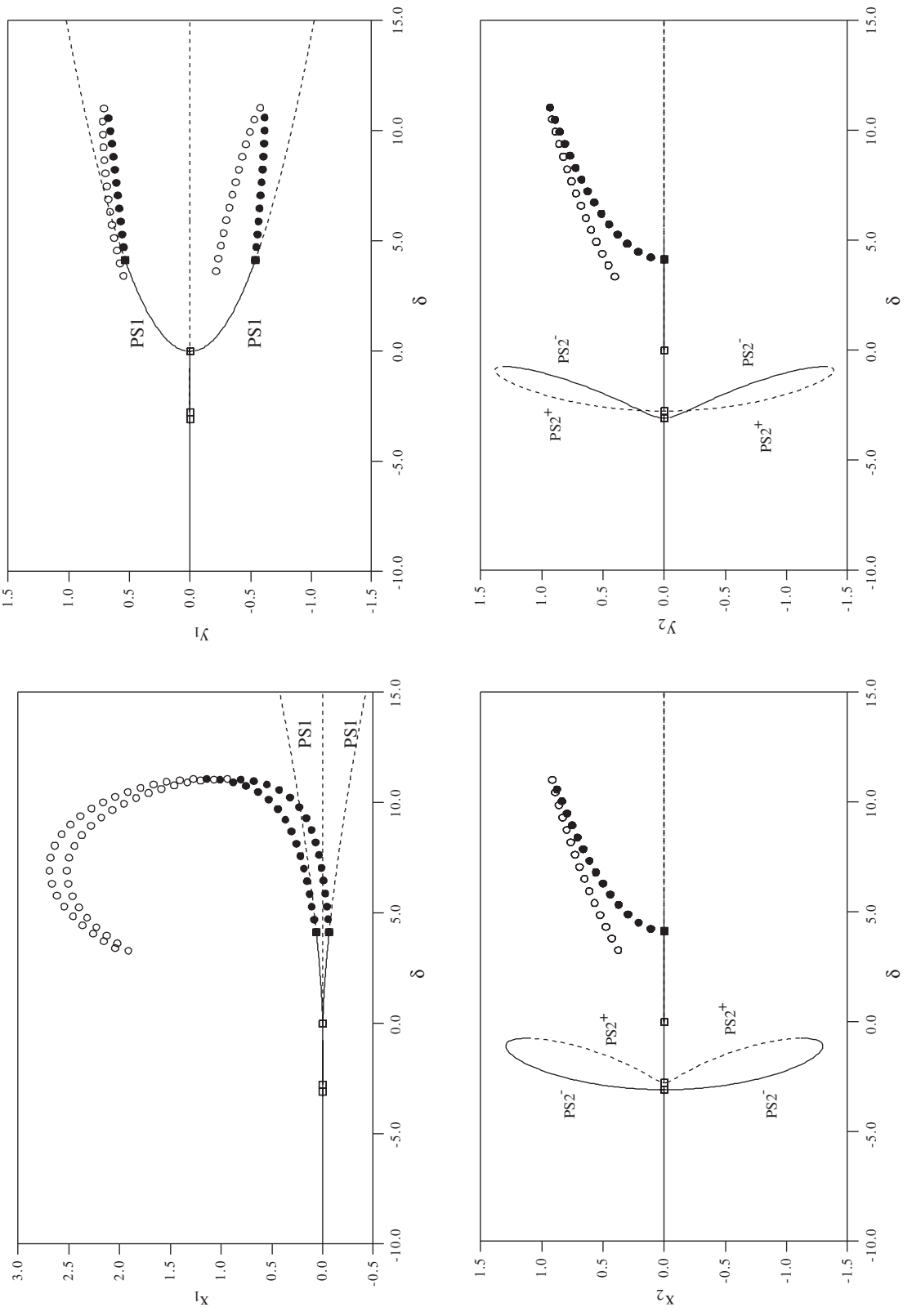

Fig. 16. Plots of coordinates versus δ for the same conditions as Fig. 15.

conditions under which energy transfer may occur from the high-frequency mode to the low-frequency mode. We will obtain similar conditions in the global analysis McDonald and Namachchivaya (2005).

Appendix A. Equations of motion for pipe conveying fluid

The system we consider consists of a uniform pipe of length L, with internal perimeter S, mass per unit length m, and flexural rigidity EI, which conveys an incompressible fluid with mass per unit length M flowing axially with velocity $U(t)$. The cross-sectional area A of the flow is assumed constant, and the fluid pressure is maintained at $\bar{p}$. The pipe, although flexible, maintains its dimensions under the effects of internal pressure and frictional drag. When undeformed, the axis of the pipe is aligned with the x-axis. Furthermore, we ignore the effects of gravity, assuming that the pipe is nominally horizontal. We shall assume that the free motions of the pipe occur in one plane, the $x-y$ plane, and we further assume that the transverse motions $y(x,t)$ are small. This system is shown in Fig. 17. Since we are interested in the post-bifurcation behavior of this system, we must include nonlinear terms. Thus, we consider the first-order nonlinearities introduced to Paidoussis and Issid's model by Holmes (1977) and Namachchivaya and Tien (1989b). These nonlinearities are due to the axial extension created by lateral motions of the pipe. Assuming Kelvin–Voigt viscoelasticity for the pipe material, the equation of motion becomes

$$\left(E^*\frac{\partial}{\partial t}+E\right)Iy^{iv}+\left\{MU^2+M\frac{\mathrm{d}U}{\mathrm{d}t}(L-x)-T_e-\frac{EA}{2L}\int_0^L(y')^2\,\mathrm{d}x-\frac{E^*A}{L}\int_0^L(y'\dot{y}')\,\mathrm{d}x\right\}y''+2MU\dot{y}'+(M+m)\ddot{y}=0.$$

For a simply supported pipe (pinned–pinned), the boundary conditions are

$$y=y''=0 \quad \text{at } x=0,\ L,$$

while for the clamped–clamped pipe, the boundary conditions are given by

$$y=y'=0 \quad \text{at } x=0,\ L.$$

The boundary conditions for pinned–clamped pipes are easy to deduce.

A.1. Nondimensionalization

We then nondimensionalize the equation by using

$$\xi=\frac{x}{L},\quad \eta=\frac{y}{L},\quad \tau=\sqrt{\frac{EI}{m+M}}\frac{t}{L^2},\quad u=\sqrt{\frac{M}{EI}}UL,\quad \bar{T}=\frac{T_eL^2}{EI},$$

$$M_r=\sqrt{\frac{M}{m+M}},\quad \bar{E}^*=\frac{E^*}{L^2}\sqrt{\frac{I}{E(m+M)}},\quad \kappa=\frac{AL^2}{2I},\quad \bar{\sigma}=\frac{E^*A}{\sqrt{EI(M+m)}}.$$

We also can write the nonlinear damping coefficient $\bar{\sigma}$ in terms of the coefficient κ as

$$\bar{\sigma}=\frac{E^*A}{\sqrt{EI(M+m)}}=\frac{A}{\sqrt{EI(M+m)}}\frac{\bar{E}^*L^2\sqrt{E(M+m)}}{\sqrt{I}}=\bar{E}^*\frac{AL^2}{I}=2\kappa\bar{E}^*.$$

The nondimensional form of the equation is then

$$\bar{E}^*\dot{\eta}^{iv}+\eta^{iv}+\left\{a_0-a_1\xi-\kappa\int_0^1(\eta')^2\,\mathrm{d}\xi-\bar{\sigma}\int_0^1(\eta'\dot{\eta}')\,\mathrm{d}\xi\right\}\eta''+a_2\dot{\eta}'+\ddot{\eta}=0, \tag{19}$$

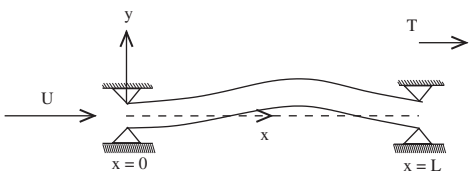

Fig. 17. A horizontal pipe conveying fluid.

where

$$a_0 = u^2 - \bar{T} + M_r\dot{u}, \quad a_1 = M_r\dot{u}, \quad a_2 = 2M_r u. \tag{20}$$

Eq. (19) is a PDE for the nondimensional vertical displacement of the pipe, $\eta(\xi,\tau)$. We will use Galerkin's method to construct an ODE for each Fourier mode. Standard Galerkin-type projections allow us to approximate this by a more tractable finite-dimensional system of dynamical systems. Suppose $\eta(\xi,\tau)$ can be approximated by

$$\bar{\eta}(\xi,\tau) = \sum_{j=1}^{n} \Phi_j(\xi) q_j(\tau), \tag{21}$$

where $\Phi_j(\xi)$ are eigenfunctions for the free undamped vibrations of a beam which satisfy the boundary conditions, and $q_j(\tau)$ is the time-dependent amplitude of the jth eigenfunction.

Using the orthogonality properties

$$\int_0^1 \Phi_j \Phi_s \,\mathrm{d}\xi \quad \begin{cases} = 0 & j \neq s, \\ \neq 0 & j = s \end{cases}$$

the relationships (obtained from integration by parts)

$$\int_0^1 \Phi_j^{iv} \Phi_s \,\mathrm{d}\xi = \int_0^1 \Phi_j'' \Phi_s'' \,\mathrm{d}\xi, \qquad \int_0^1 \Phi_j'' \Phi_s \,\mathrm{d}\xi = -\int_0^1 \Phi_j' \Phi_s' \,\mathrm{d}\xi$$

and defining

$$B = b_{sj} = \int_0^1 \Phi_j'(\xi)\Phi_s(\xi)\,\mathrm{d}\xi, \quad C = c_{sj} = \int_0^1 \Phi_j''(\xi)\Phi_s(\xi)\,\mathrm{d}\xi,$$
$$D = d_{sj} = \int_0^1 \xi\Phi_j''(\xi)\Phi_s(\xi)\,\mathrm{d}\xi, \quad \delta_{sj} = \int_0^1 \Phi_j(\xi)\Phi_s(\xi)\,\mathrm{d}\xi,$$

we obtain a pair of second-order finite-dimensional ODEs for the time-dependent amplitude coefficients in matrix form

$$\ddot{\mathbf{q}} + (\bar{E}^* \Lambda + a_2 B)\dot{\mathbf{q}} + (\Lambda + a_0 C - a_1 D)\mathbf{q} + f(\mathbf{q}, \dot{\mathbf{q}}) = \mathbf{0},$$

where $\Lambda = \mathrm{diag}\{\lambda_1^4, \lambda_2^4, \ldots, \lambda_n^4\}$, and the cubic nonlinear terms are given by $f(\mathbf{q}, \dot{\mathbf{q}})$.

References

Ariaratnam, S.T., Namachchivaya, N. Sri., 1986. Dynamic stability of pipes in pulsating flow. Journal of Sound and Vibration 107, 215–230.

Ashley, H., Haviland, G., 1950. Bending vibrations of pipe line containing flowing fluid. ASME Journal of Applied Mechanics 17, 229–232.

Benjamin, T.B., 1961. Dynamics of a system of articulated pipes conveying fluid; Part I: theory. Proceedings of the Royal Society (London): Series A 261, 457–486.

Ch'ng, E., 1978. A theoretical analysis of nonlinear effect on the flutter and divergence of a tube conveying fluid. Technical Report AMS Report No. 1343 (revised), Department of Mechanical and Aerospace Engineering, Princeton University.

Doedel, E.J., Champneys, A.R., Fairgrieve, T.F., Kuznetsov, Y.A., Sandstede, B., Wang, X., 1997. AUTO97: Continuation and Bifurcation Software for Ordinary Differential Equations. Concordia University, Montreal, Canada.

Feodos'ev, V.P., 1951. Vibrations and stability of a pipe when liquid flows through it. Inzhenernyi Sbornik 10, 169–170.

Holmes, P.J., 1977. Bifurcations to divergence and flutter in flow-induced oscillations: a finite dimensional analysis. Journal of Sound and Vibration 53, 471–503.

Housner, G.W., 1952. Bending vibrations of a pipe line containing flowing fluid. Journal of Applied Mechanics 20, 205–208.

McDonald, R., Namachchivaya, N. Sri., 2005. Pipes conveying pulsating fluid near a 0:1 resonance: global bifurcations. Journal of Fluids and Structures, in press, doi:10.1016/j.jfluidstructs.2005.07.015.

McDonald, R., Murdouck, J.A., Namachchivaya, N. Sri., 1999. Normal forms for nonlinear Hamiltonian systems with weak periodic perturbations. Journal of Dynamics and Stability of Systems 14, 187–211.

Meyer, K.R., Hall, G.R., 1992. Introduction to Hamiltonian Dynamical Systems and the N-Body Problem. Springer, New York.

Nagata, W., Namachchivaya, N. Sri., 1998. Bifurcations in gyroscopic systems with an application to rotating shafts. Proceedings of the Royal Society: Series A 454, 543–585.

Namachchivaya, N. Sri., 1989. Nonlinear dynamics of supported pipe conveying pulsating fluid, Part I: subharmonic resonance. International Journal of Non-linear Mechanics 24, 185–196.

Namachchivaya, N. Sri., Tien, W.M., 1989a. Nonlinear dynamics of supported pipe conveying pulsating fluid, Part II: combination resonance. International Journal of Non-linear Mechanics 24, 197–209.

Namachchivaya, N. Sri., Tien, W.M., 1989b. Bifurcation behavior of nonlinear pipes conveying pulsating flow. Journal of Fluids and Structures 3, 609–629.

Niordson, F.I., 1953. Vibrations of a cylindrical tube containing flowing fluid. Kungliga Tekniska Hogskolans Handlingar 73, 19–53.

Paidoussis, M.P., Issid, N.T., 1974. Dynamic stability of pipes conveying fluid. Journal of Sound and Vibration 33, 267–294.

Paidoussis, M.P., Li, G.X., 1993. Pipes conveying fluid: a model dynamical problem. Journal of Fluids and Structures 7, 137–204.

Paidoussis, M.P., Sundararajan, C., 1975. Parametric and combination resonance of pipe conveying pulsating fluid. Journal of Applied Mechanics 42, 780–784.

Rousselet, J., Herrmann, G., 1977. Flutter of articulated pipes at finite amplitude. Journal of Applied Mechanics 44, 154–158.

Thurman Jr., A.L., Mote, C.D., 1969. Nonlinear oscillation of a cylinder containing a flowing fluid. ASME Journal of Engineering for Industry 91, 1147–1155.